proba-v

QUARTERLY IMAGE QUALITY REPORT

IQR#021

Reporting period from 16/09/2018 to 15/03/2019

Reference: ***PROBA-V_D9_QIR-021_2019-Q1_v1.0***
Author(s): Sindy Sterckx, Stefan Adriaensen, Iskander Benhadj, Erwin Wolters
Version: 1.0
Date: 20/03/2019

DOCUMENT CONTROL

Signatures

Author(s)	Sindy Sterckx, Stefan Adriaensen, Erwin Wolters, Iskander Benhadj
Reviewer(s)	Dennis Clarijs
Approver(s)	Dennis Clarijs
Issuing authority	VITO N.V.

Change record

Release	Date	Pages	Description	Editor(s)/Reviewer(s)
1.0	20/03/2019	All	Initial version	

TABLE OF CONTENT

1. Radiometric Image Quality

1.1. Summary

Due the Antarctica acquisitions, and related disabling of the sun bathing mode, the instrument temperature for VNIR detector has increased significantly from about -3° in October 2018 to about 2° in January 2019. Since the increase in instrument temperature the DCC calibration results showed a sudden increase in the NIR band results of 1 to 1.5%. This increase is also visible in the Libya-4 desert results and the lunar calibration results for RED and NIR bands. By February 18, 2019 the Antarctica acquisitions have been finished and the sun bathing mode has been re-enabled which resulted in a decrease again of the instrument temperature. The DCC NIR band calibration results are now (mid-March 2019) at about the same level as before the start of the Antarctica acquisition. Some lunar calibration acquisitions are scheduled for the coming days to verify if the calibration results are back at the normal level. It should be noticed that in the radiometric sensor model there is no temperature dependency included for the absolute calibration coefficient. Currently no updates to the absolute ICP file were performed to mitigate or to correct for the impact of the temporary temperature increase on the radiometric signal.

The yaw maneuver data of summer 2018 have been fully analyzed; summary of the results is given in this report. A short paper about the yaw maneuver will be published in the GSICS quarterly newsletter.

During Q1 of 2019 no new bad pixel was identified.

1.2. Assessment of the radiometric accuracy

1.2.1. Absolute radiometric accuracy

The absolute radiometric calibration requirement for PROBA-V specifies a 5 % absolute accuracy. This requirement is assessed through vicarious calibration over Libya-4 desert site and Rayleigh calibration zones.

1.2.1.1. Libya-4 desert calibration

Methodology

The nominal approach for assessing the absolute radiometric accuracy relies on the comparison between cloud-free TOA reflectance as measured over the Libya-4 desert site by PROBA-V and the modelled TOA reflectance values, following the approach described in [LIT1]. Validation of the approach using various satellite data (i.e. AQUA-MODIS, MERIS, AATSR, PARASOL, SPOT-VGT) has shown that absolute calibration over the Libya-4 desert is achievable with this approach with an accuracy of 3% [LIT1, LIT2].

Results

In Figure1, Figure3 and Figure 5 the monthly averaged results ($avg(\rho_{TOA}^{k,ProbaV(Acom)}/\rho_{TOA}^{k,model})$) and its standard deviation are given for respectively LEFT, CENTER and RIGHT camera.
The individual area-averaged results are given in Figure2, Figure4 and Figure 6 with a 3 % error bar (as expected uncertainty for an individual result) for respectively VNIR and SWIR strips.

Results are obtained based on the **Collection 1** ICP files.

Since October 2018 a degradation model is no longer applied to the SWIR absolute calibration coefficients as the current linear model resulted in an overcorrection of the degradation in the SWIR.

Some slight increase in the RED and NIR band calibration results is observed in the period November 2018 – February 2019 which is thought to be linked to the increase in the instrument temperature due to disabling of the sun bathing mode in frame of the continuous Antarctica acquisitions.

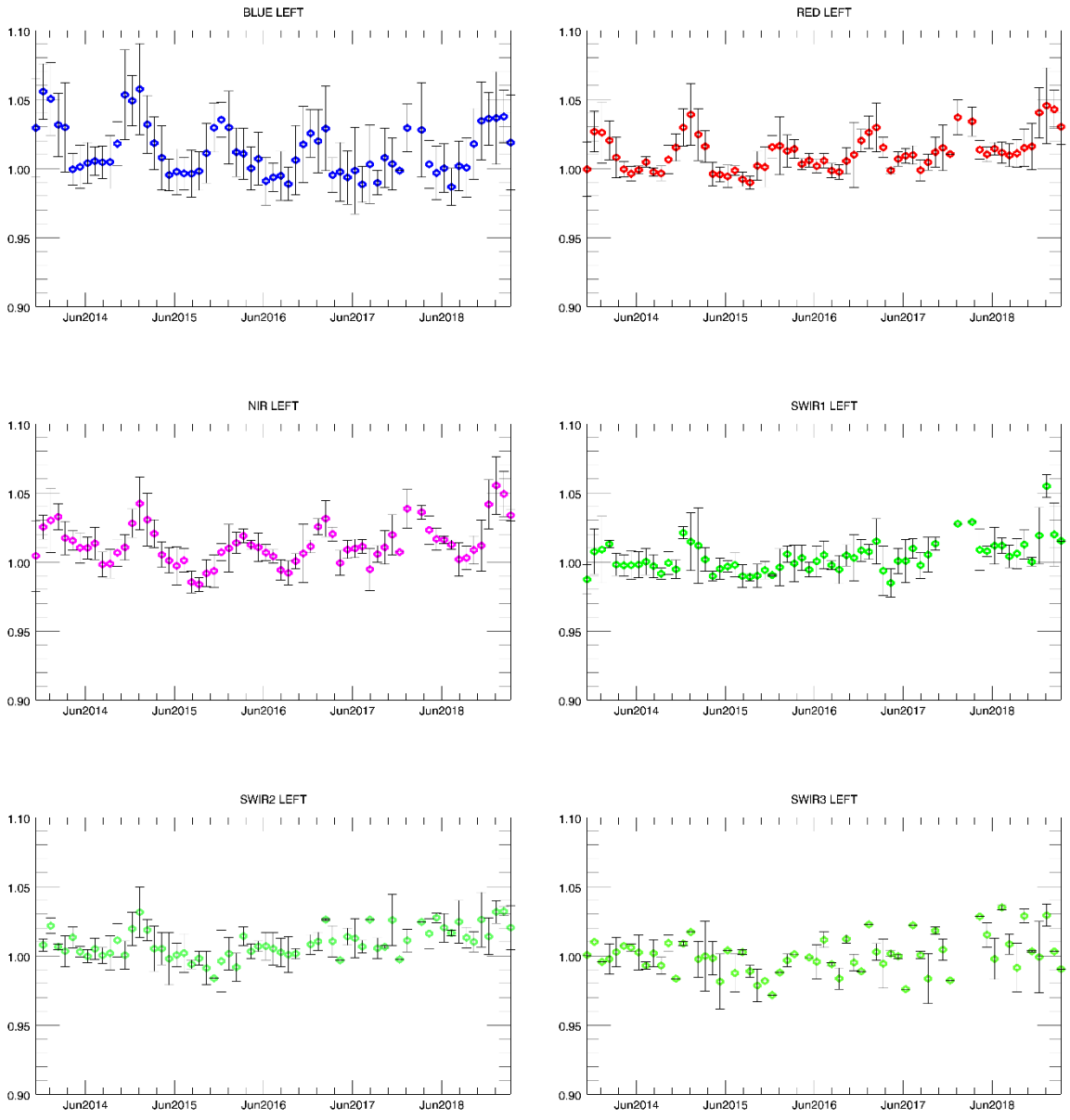

Figure 1. Libya-4 desert calibration results: LEFT monthly averaged results (Collection 1)

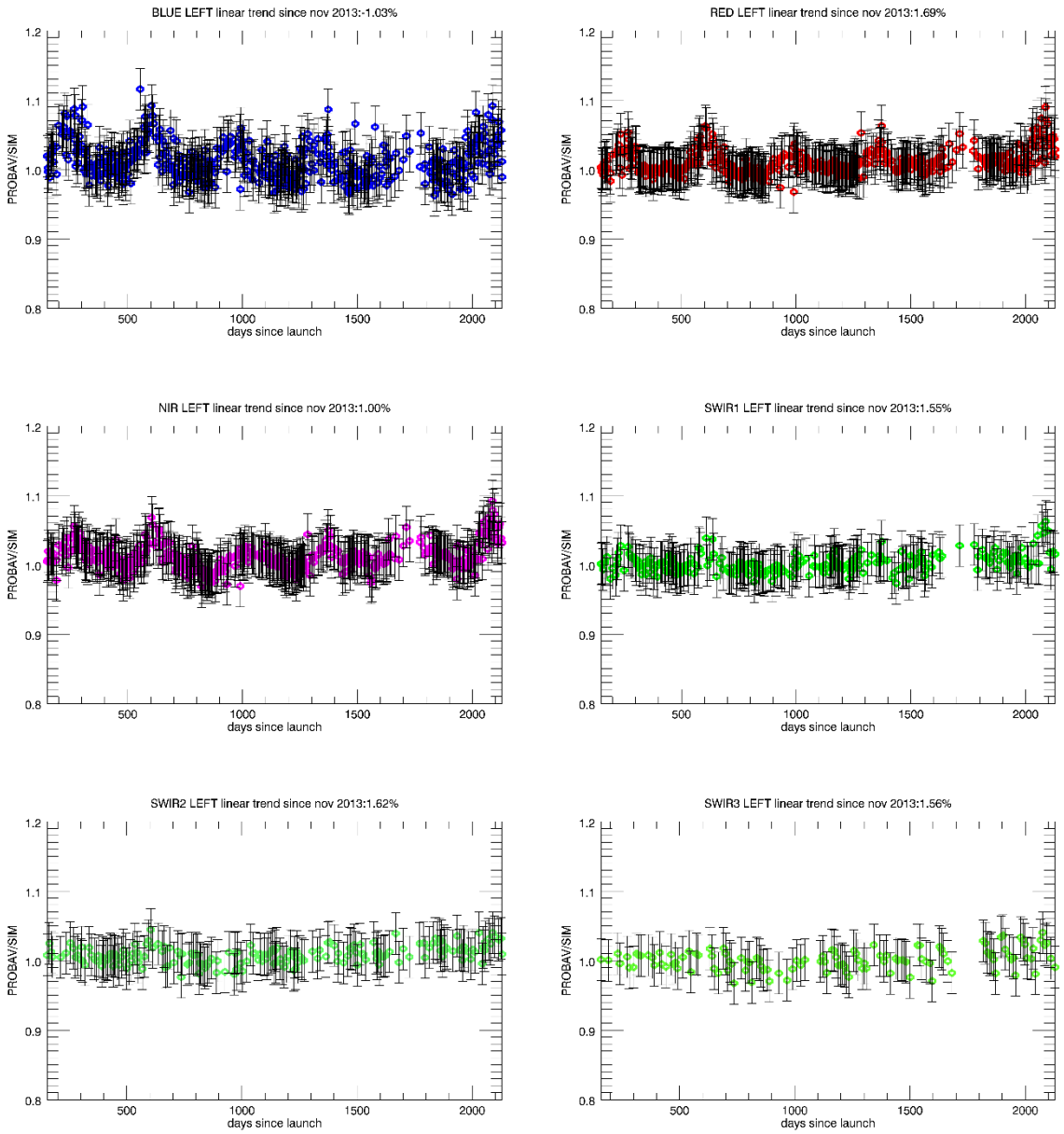

Figure 2. Libya-4 desert calibration results: LEFT individual results (Collection 1)

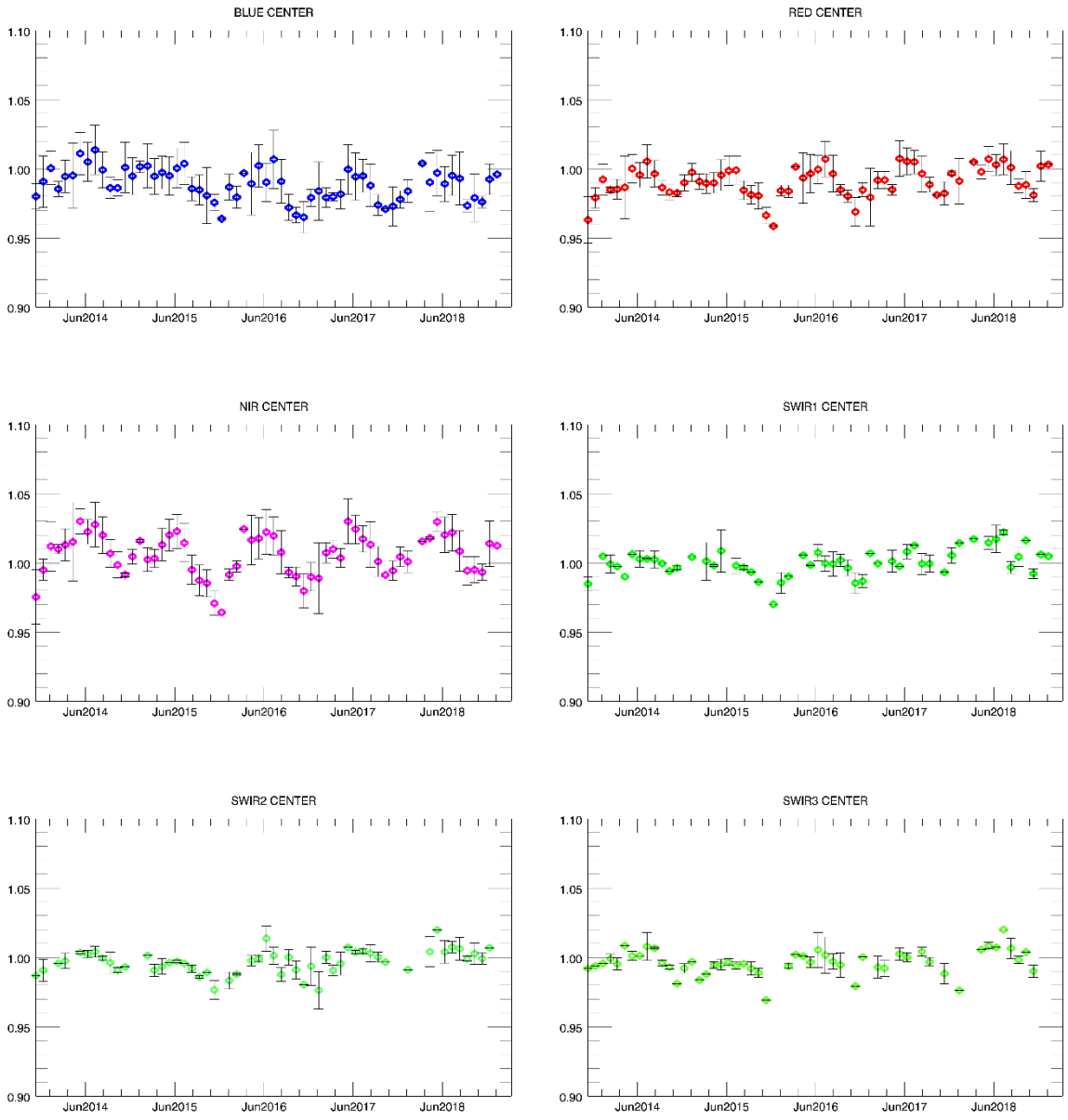

Figure 3. Libya-4 desert calibration results: CENTER monthly averaged results (Collection 1)

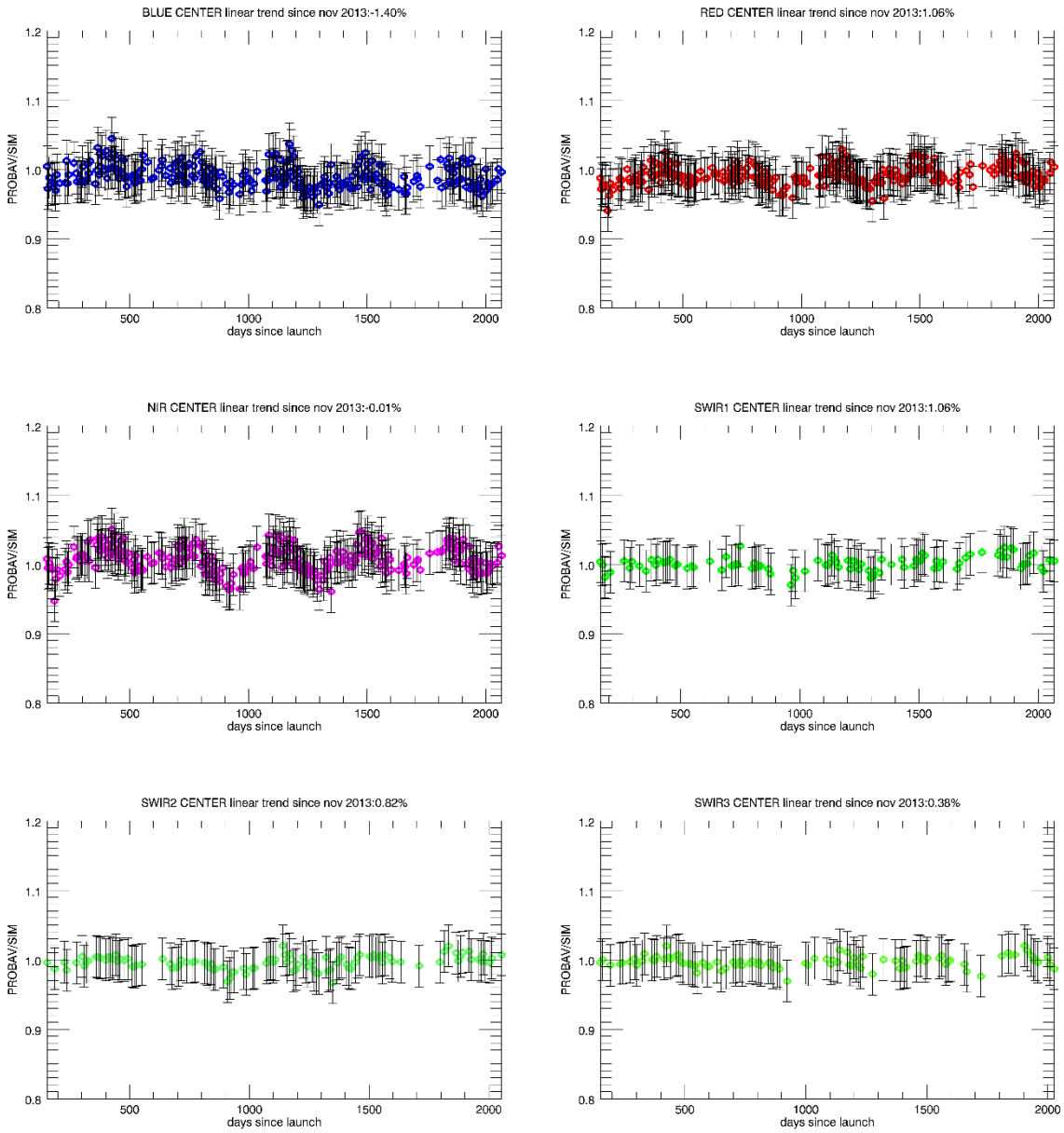

Figure 4. Libya-4 desert calibration results: CENTER individual results (Collection 1)

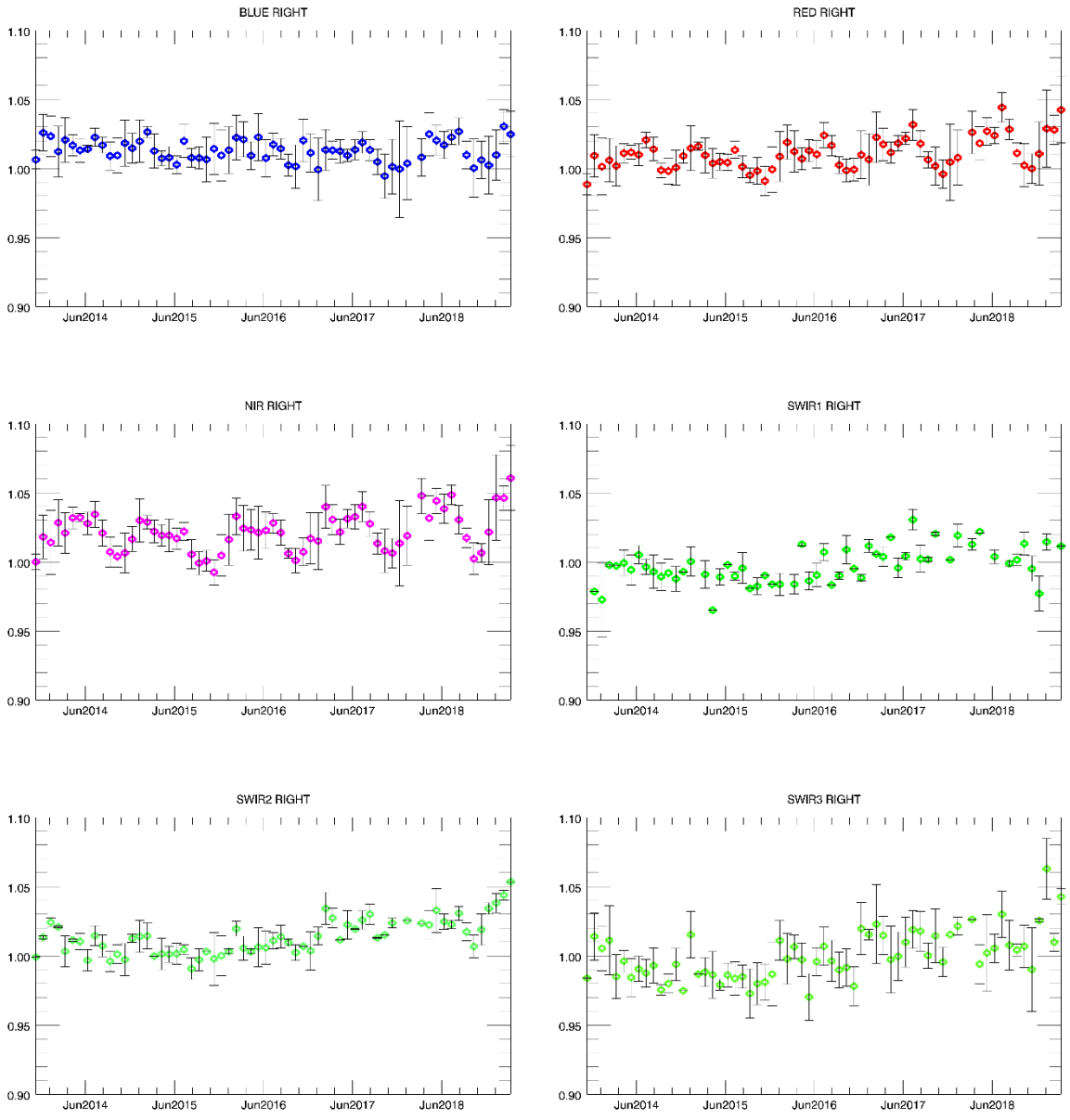

Figure 5. Libya-4 desert calibration results: RIGHT monthly averaged results (Collection 1)

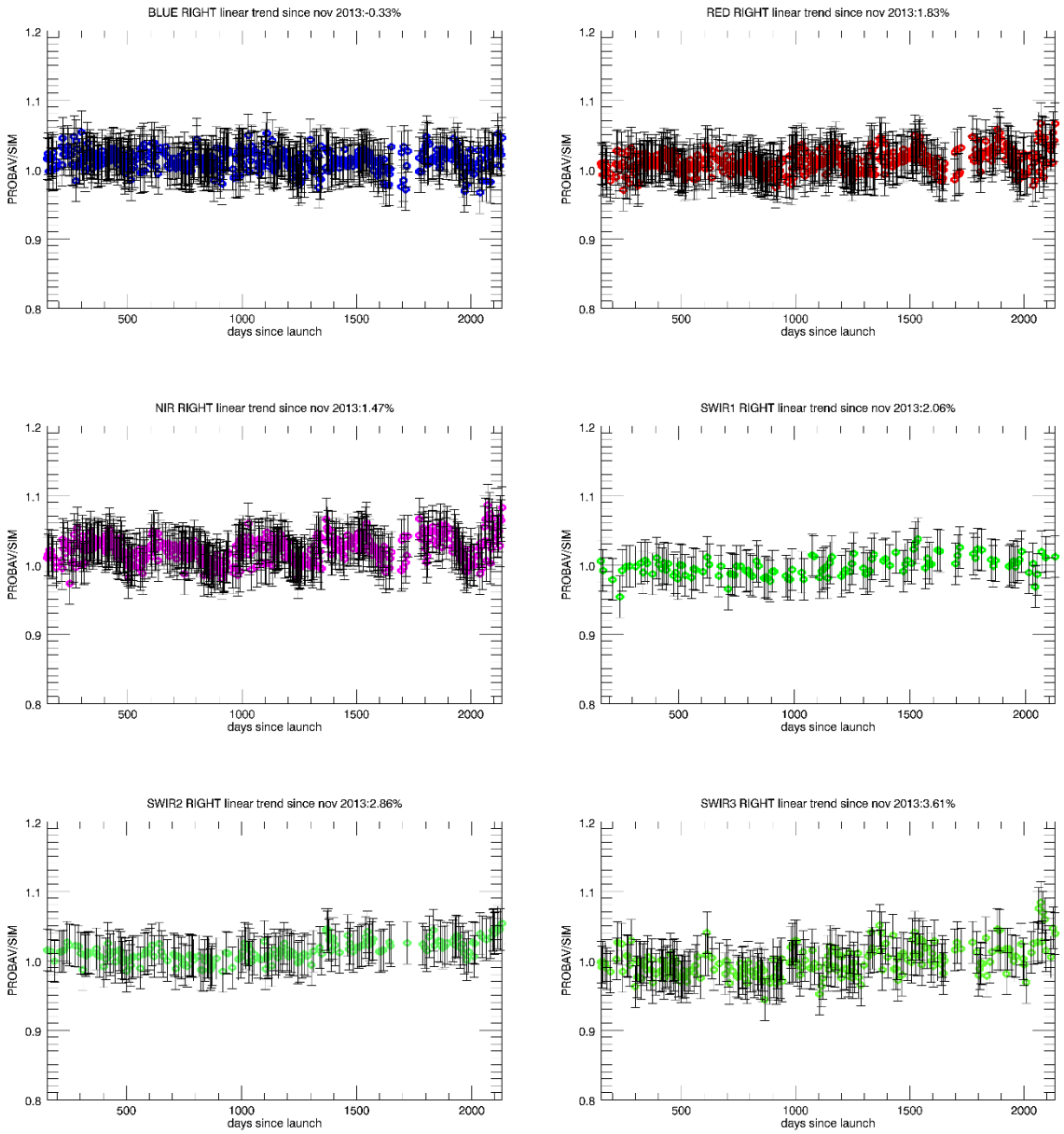

Figure 6. Libya-4 desert calibration results: RIGHT individual results (Collection 1)

1.2.1.2. Rayleigh calibration

Methodology

The Rayleigh calibration approach is an absolute calibration method for BLUE and RED bands. The primary assumption of the approach is that the ocean does not contribute to the Top-Of-Atmosphere (TOA) signal in the NIR. The contribution of aerosol scattering is derived from the ***NIR reference band*** where molecular scattering is negligible. The aerosol content estimated from the NIR band is then transferred to the BLUE and RED band to model the TOA radiance with a radiative transfer code. The simulated radiance values are then compared with the measured values.

Results

The scene averaged Rayleigh results ($(\rho_{TOA}^{k,ProbaV(Acom)}/\rho_{TOA}^{k,model})$) (with a 4 % error bar as rough indication of uncertainty of one individual result) obtained since January 2014 for LEFT, CENTER and RIGHT camera are given in respectively Figure 7, Figure 8 and Figure 9.

Results are obtained using the **Collection 1 ICP** files.

No significant trend is visible in the Rayleigh calibration results.

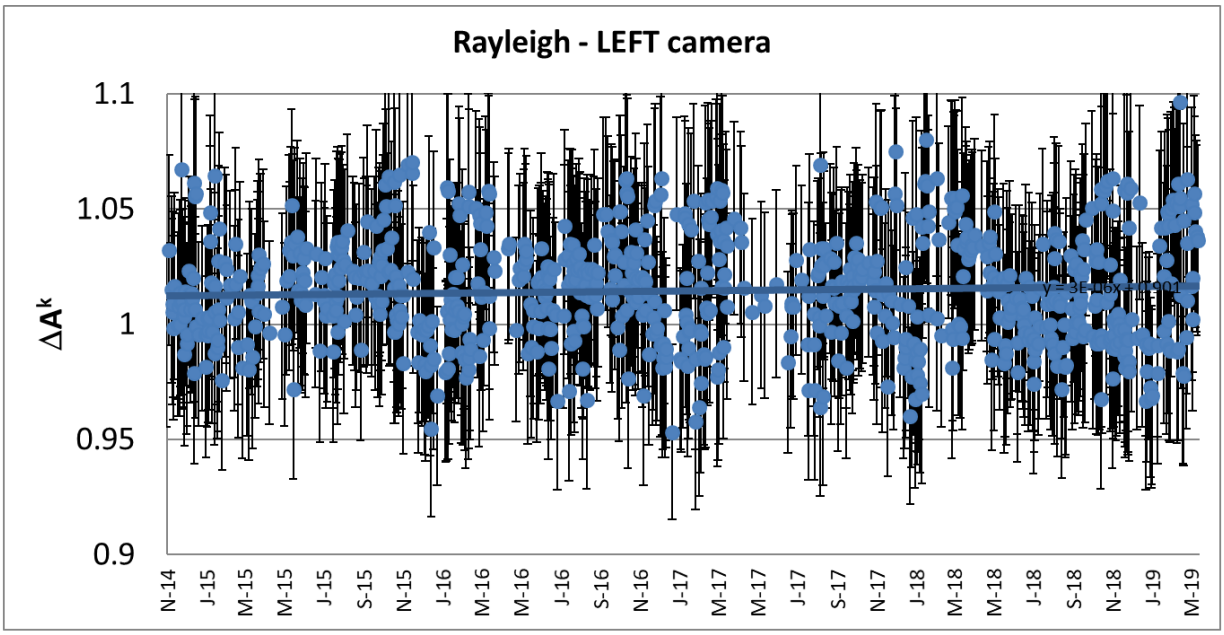

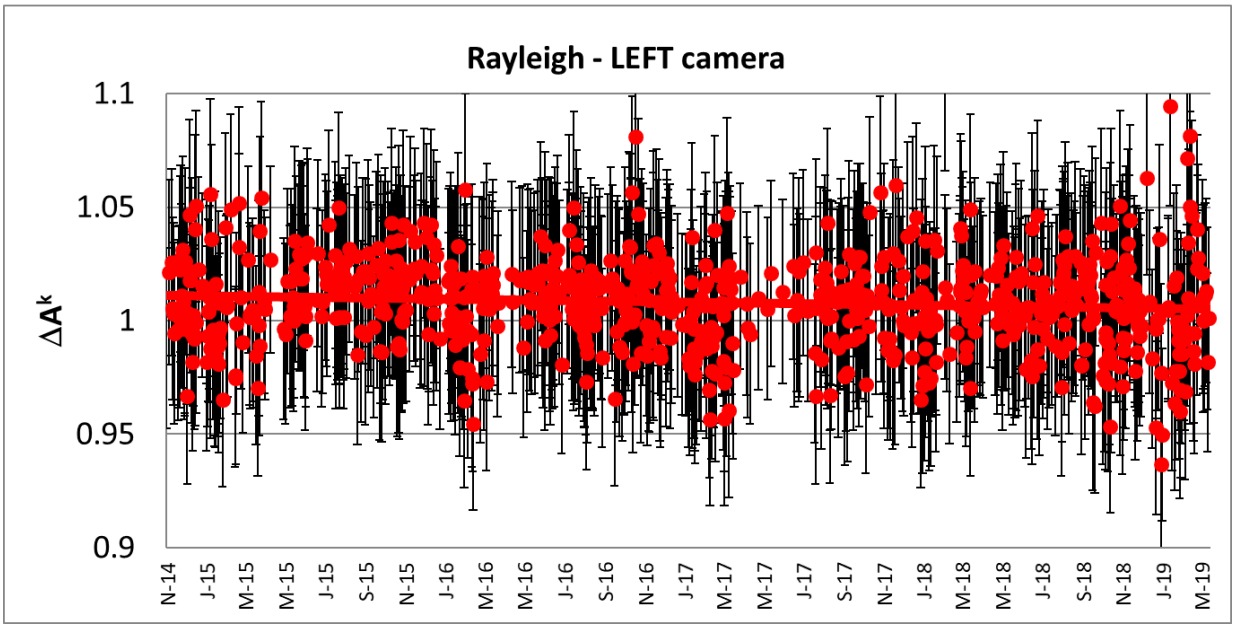

Figure 7. Rayleigh absolute calibration results: LEFT camera (Collection 1)

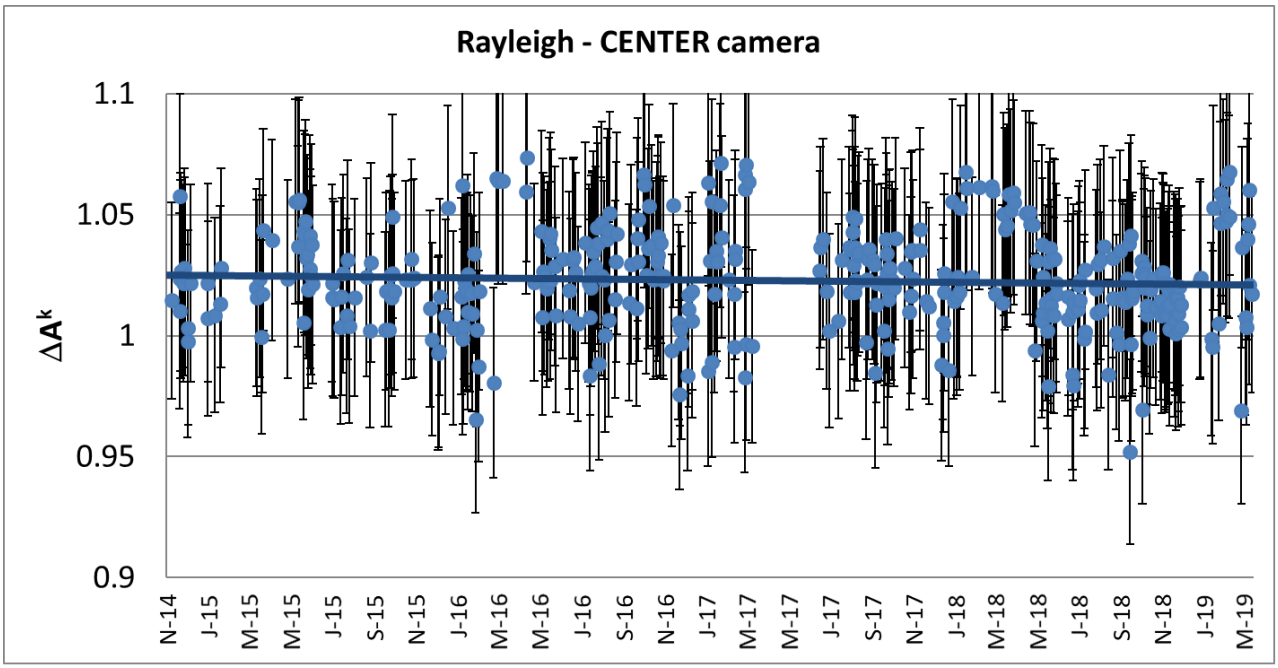

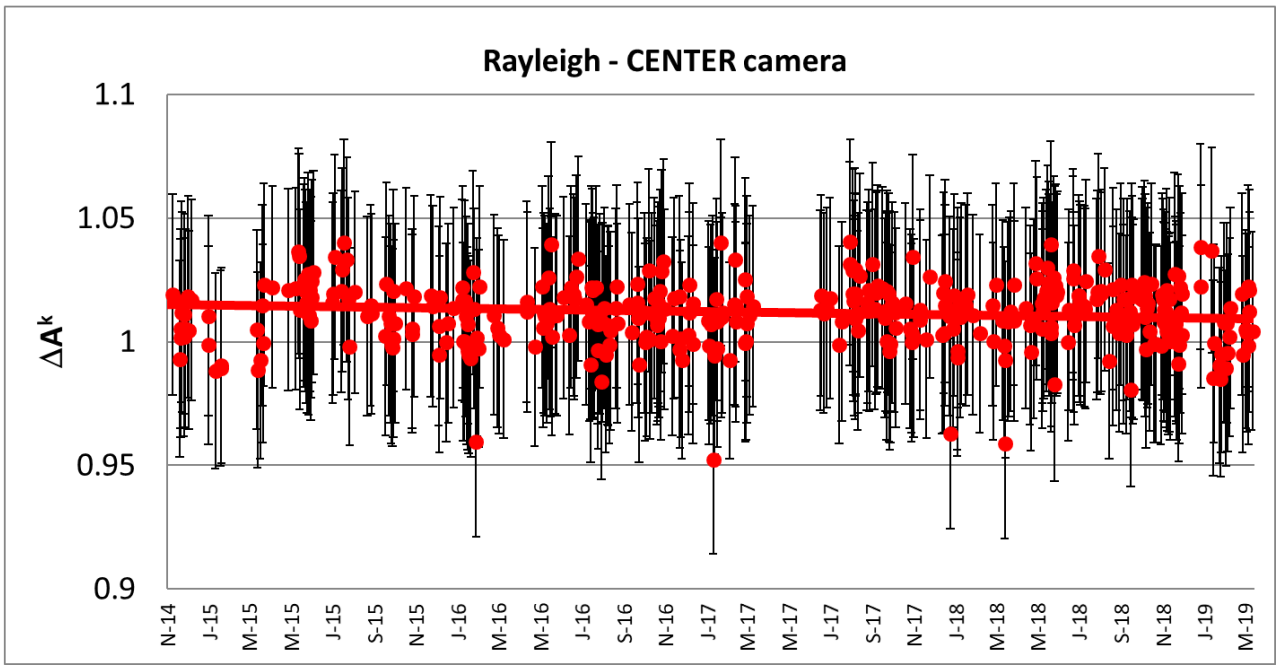

Figure 8. Rayleigh absolute calibration results: CENTER camera (Collection 1)

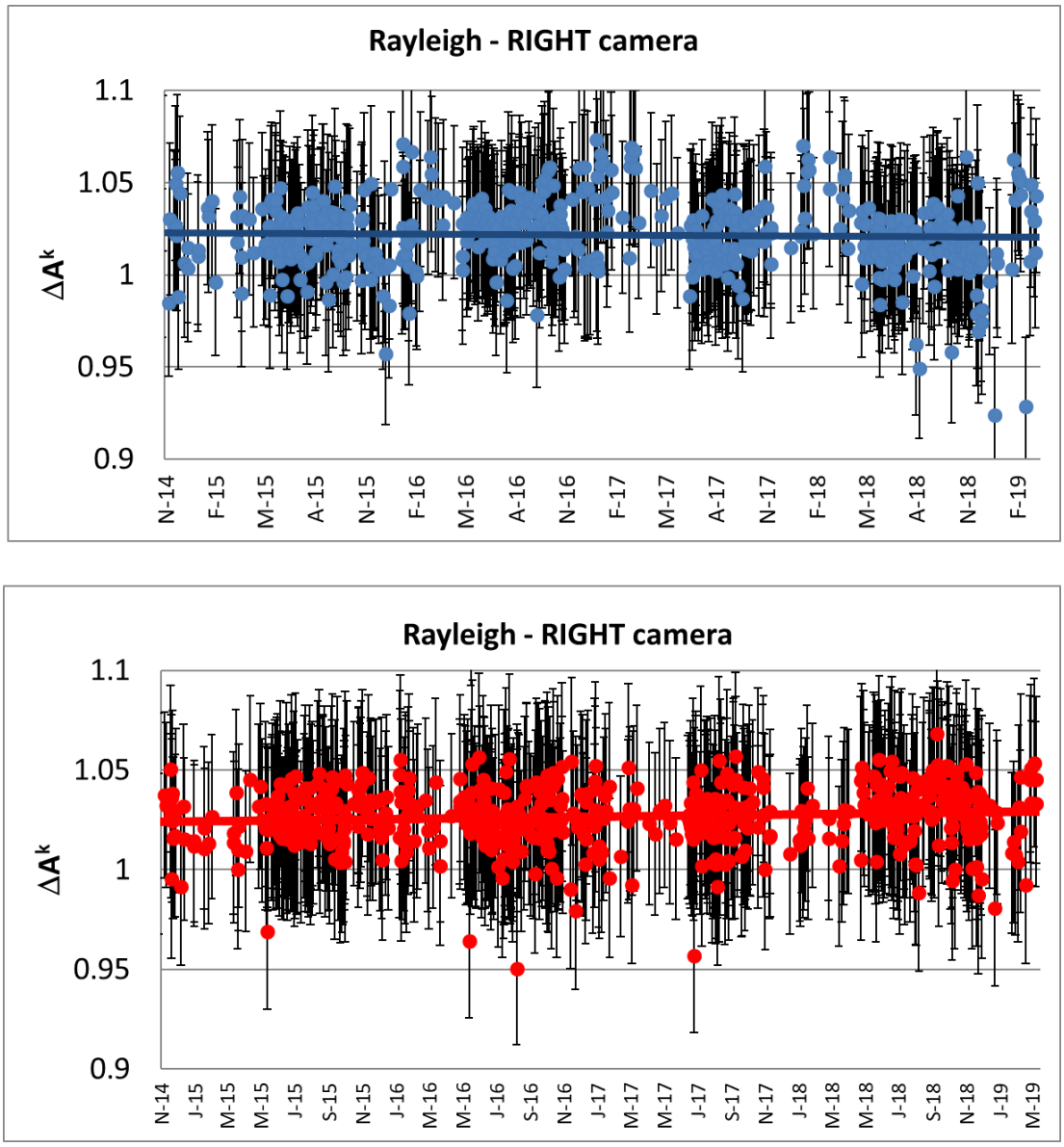

Figure 9. Rayleigh absolute calibration results: RIGHT camera (Collection 1)

1.2.2. Inter-band radiometric accuracy

The inter-band radiometric calibration requirement for PROBA-V specifies a 3 % inter-band accuracy. This requirement is assessed through vicarious calibration over deep convective clouds.

1.2.2.1. Calibration over deep convective clouds (DCC)

Methodology

The DCC approach is an inter-band calibration method. It makes use of bright, thick, high altitude, convective clouds over oceanic sites. Their reflective properties are spectrally flat in visible and near-infrared and the only contributions to the observed signal are from the cloud reflectance, molecular scattering and ozone absorption which can be modelled with a radiative transfer code.
The cloud reflectance in the non-absorbing VNIR bands is mainly sensitive to the cloud optical thickness. The DCC method uses the TOA reflectance in the 'reference' RED band to estimate cloud optical thickness assuming a fixed ice particle model. The derived cloud optical thickness is then used to model using a radiative transfer code the TOA reflectance for the BLUE and NIR band.

The method is not suited for the SWIR band as clouds are no longer spectrally uniform in this spectral region.

Results

The DCC inter-band calibration is defined by reference to the used RED reference band. The average DCC inter-band calibration result per month (from March 2015 to March 2019) is given in Figure 10 for all cameras using the **collection 1 ICP files**.

Similarly as for the Libya-4 results the DDC calibration results show a sudden increase in the NIR band results for the period November 2018 – February 2019 which is thought to be linked to the increase in the instrument temperature due to disabling of the sun bathing mode in frame of the continuous Antarctica acquisitions. By February 27, 2019 the Antarctica acquisitions have been finished and the sun bathing mode has been re-enabled which resulted in a decrease again of the instrument temperature. The DCC NIR band calibration results are now (mid-March 2019) almost at about the same level as before the start of the Antarctica acquisition.

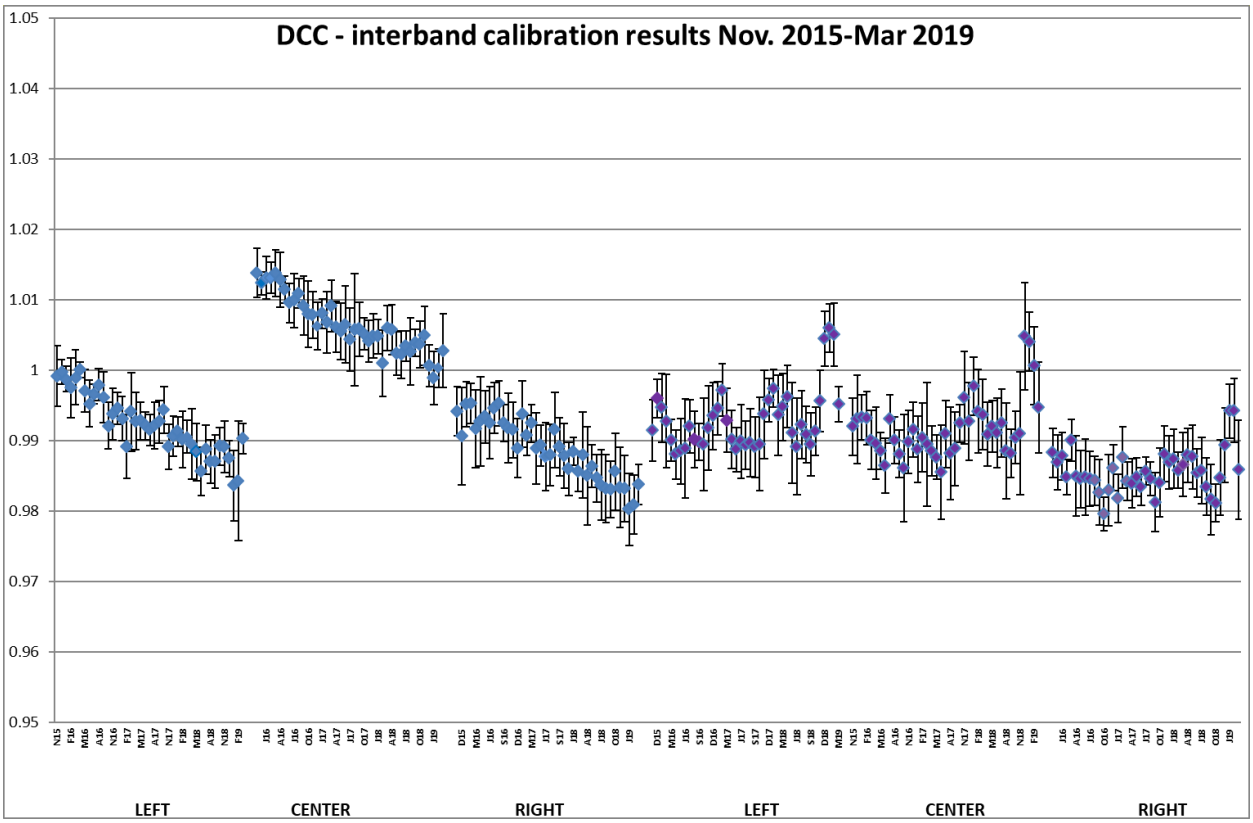

Figure 10. DCC inter-band calibration results: LEFT, CENTER and RIGHT camera

1.2.3. PROBA-V Multi-temporal radiometric accuracy

1.2.3.1. Degradation model

Since October 2018 a degradation model is no longer applied to the SWIR absolute calibration coefficients as the current linear model resulted in an overcorrection of the degradation in the SWIR. Investigation for the implementation of a non-linear degradation model to take into account the asymptotic degradation trend is on-going.

In Table 1 the applied degradation model correction is given. This linear degration model is being applied for collection 1 since start of the operational phase (i.e. October 2013). A re-evaluation of the coefficients of the SWIR degradation model was performed in summer 2017. Since Jan 2018 a degradation model is no longer applied to the RIGHT SWIR strips. From October 2018 onwards, absolute calibration coefficients for the SWIR strips are not updated.

Table 1 SWIR degradation model: applied linear trend/month

	Degradation model ICP			
	Start- aug 2017	Sept 2017-Dec 2018	Jan 2018-Sept 2018	Oct 2018-..
SWIR1 LEFT	-0.087	-0.087	-0.087	NA
SWIR2 LEFT	-0.104	-0.104	-0.104	NA
SWIR3 LEFT	-0.097	-0.097	-0.097	NA
SWIR1 CENTER	-0.093	-0.093	-0.093	NA
SWIR2 CENTER	-0.092	-0.092	-0.092	NA
SWIR3 CENTER	-0.086	-0.086	-0.086	NA
SWIR1 RIGHT	-0.106	-0.077	NA	NA
SWIR2 RIGHT	-0.143	-0.122	NA	NA
SWIR3 RIGHT	-0.122	-0.078	NA	NA

A degradation model is used to update the absolute calibration coefficients of the LEFT and RIGHT BLUE since May 2017. A re-evaluation of the coefficients of the degradation model was performed in summer 2017. Since then no changes have been made to the model. In Table 2 the coefficients are given.

Table 2 Degradation model BLUE LEFT and CENTER camera: applied linear trend/month

	Linear trend/month (%)	
	Degradation model ICP	Degradation model ICP
STRIP	May 2017-aug 2017	since sept 2017
BLUE LEFT	-0.028	-0.036
BLUE CENTER	-0.011	-0.034

1.2.3.2. Lunar calibration

The Lunar calibration results for the VNIR CENTER camera bands, normalised to June 2013, are given in Figure 11. The results are given based on the **collection 1 ICP** files.

Similarly, as observed over Libya-4 and DCC the RED and NIR lunar calibration results show an increase in responsivity for the RED and NIR bands for the acquisitions performed from November till February 2019 which is probably caused by the increased temperature. Some lunar calibration acquisitions are scheduled for the coming days to verify if the calibration results are back at the normal level since the dropping of the temperature.

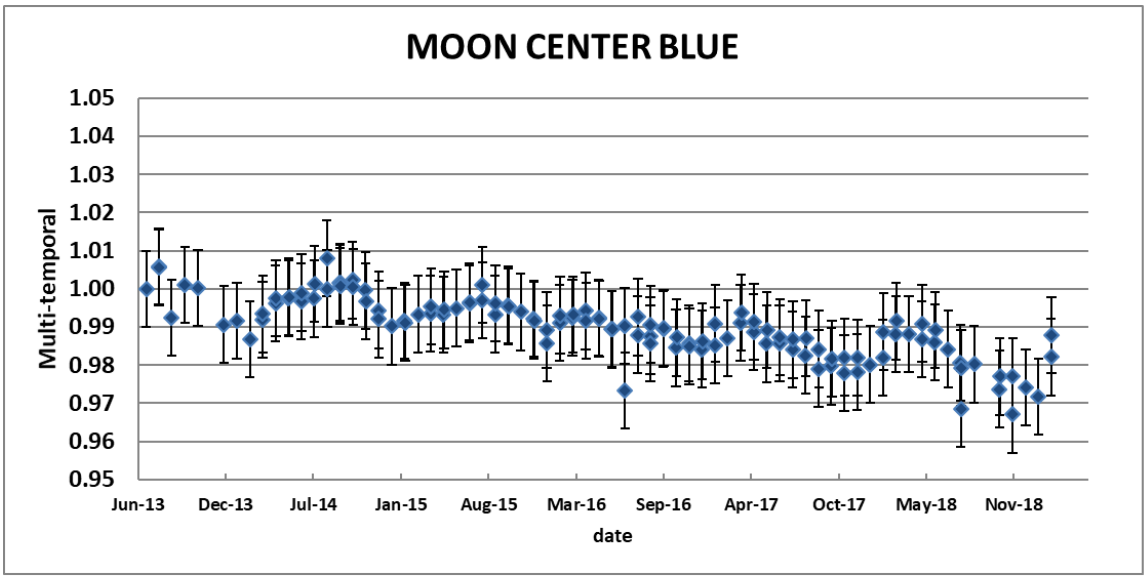
MOON CENTER BLUE
Multi-temporal
1.05
1.04
1.03
1.02
1.01
1.00
0.99
0.98
0.97
0.96
0.95
Jun-13
Dec-13
Jul-14
Jan-15
Aug-15
Mar-16
Sep-16
Apr-17
Oct-17
May-18
Nov-18
date

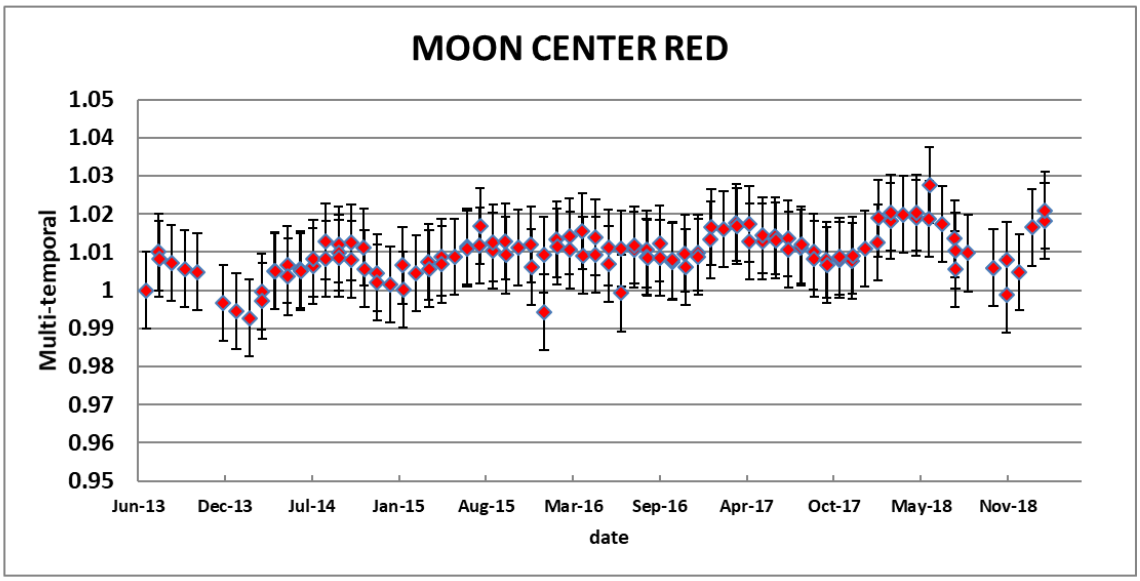
MOON CENTER RED
Multi-temporal
1.05
1.04
1.03
1.02
1.01
1
0.99
0.98
0.97
0.96
0.95
Jun-13
Dec-13
Jul-14
Jan-15
Aug-15
Mar-16
Sep-16
Apr-17
Oct-17
May-18
Nov-18
date

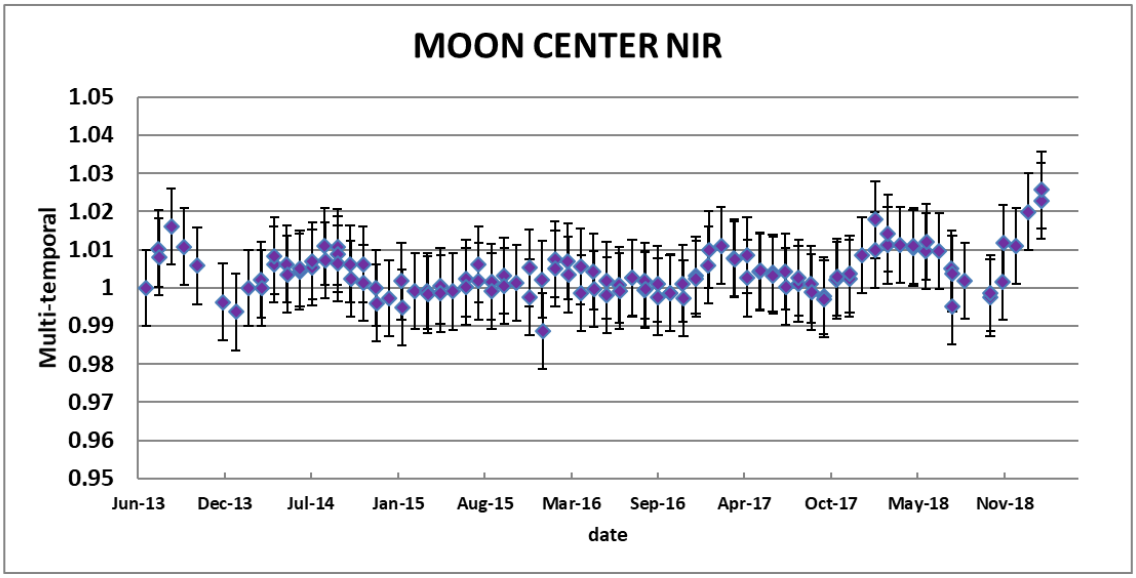
MOON CENTER NIR
Multi-temporal
1.05
1.04
1.03
1.02
1.01
1
0.99
0.98
0.97
0.96
0.95
Jun-13
Dec-13
Jul-14
Jan-15
Aug-15
Mar-16
Sep-16
Apr-17
Oct-17
May-18
Nov-18
date

Figure 11. Lunar Calibration results CENTER camera normalised to June 2013 (collection 1 ICP files)

1.2.3.3. Libya-4 VS Moon

As mentioned in previous report degradation trends observed in the Lunar calibration results for the center SWIR2 strip are less significant than these observed in the desert calibration results. In the frame of the ESA's 'Lunar Irradiance Measurements of the Moon' project VITO is working on an improved lunar model. A reprocessing of the PROBA-V lunar calibration results based on the improved model is foreseen for the near future. It is expected that this will give us a better insight in the actual degradation trend.

1.3. Dark current

1.3.1. Methodology

- Monthly difference plots :
  - All dark current results obtained during a period of one month for observations performed with a long integration time are averaged per pixel. This gives for each pixel the monthly averaged dark current, expressed **in LSB/s**, and its standard deviation.
  - The dark current results and its standard deviation expressed in LSB/s are converted to **LSB** using a maximum Integration Time for nominal acquisitions. For VNIR strips **0.006s** is used. For SWIR strips **0.02s.**
  - The differences between months (i.e. Month3-Month2, Month2-Month1) are calculated. This is done for both the dark current and the stdev. Differences are visualized in plots in blue the dark current difference in LSB is plotted, in red the standard deviation difference. This latter is an indicator of changes in the dark current noise between months.

As mentioned in the previous quarterly report (IQR#005) the integration time used for the SWIR dark current acquisitions has been decreased from 3s to 0.2 s since 2015.

1.3.2. VNIR results

Monthly difference plots for VNIR dark currents are given Figure 12, *Figure 13* and *Figure 14* for respectively LEFT, CENTER and RIGHT camera.

Dark current differences for the VNIR bands are well below 1 DN.

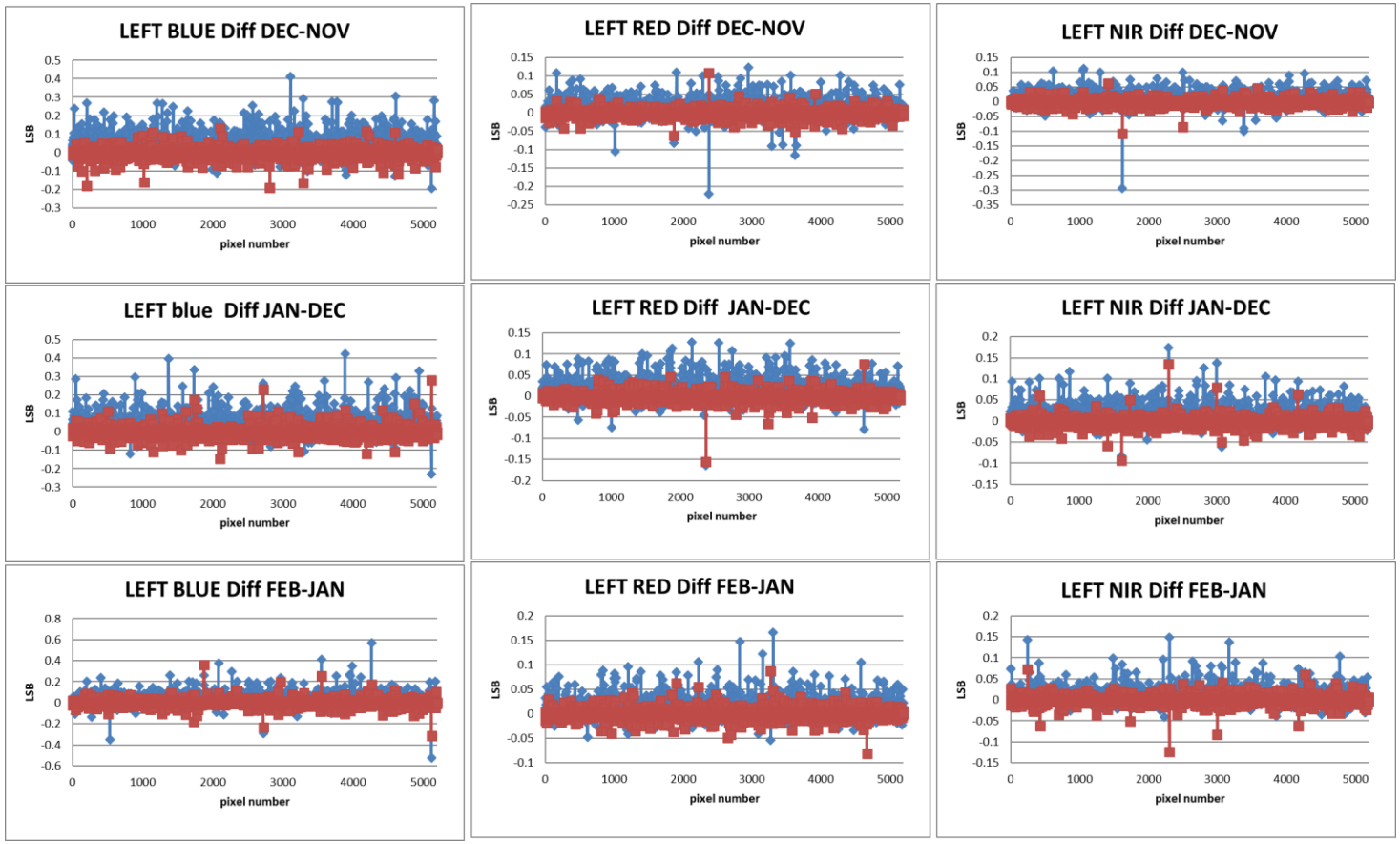

Figure 12. LEFT camera VNIR: Monthly difference (NOV 2018-FEB2019) in dark current (Blue) and standard deviation (Red) of the monthly averaged results.

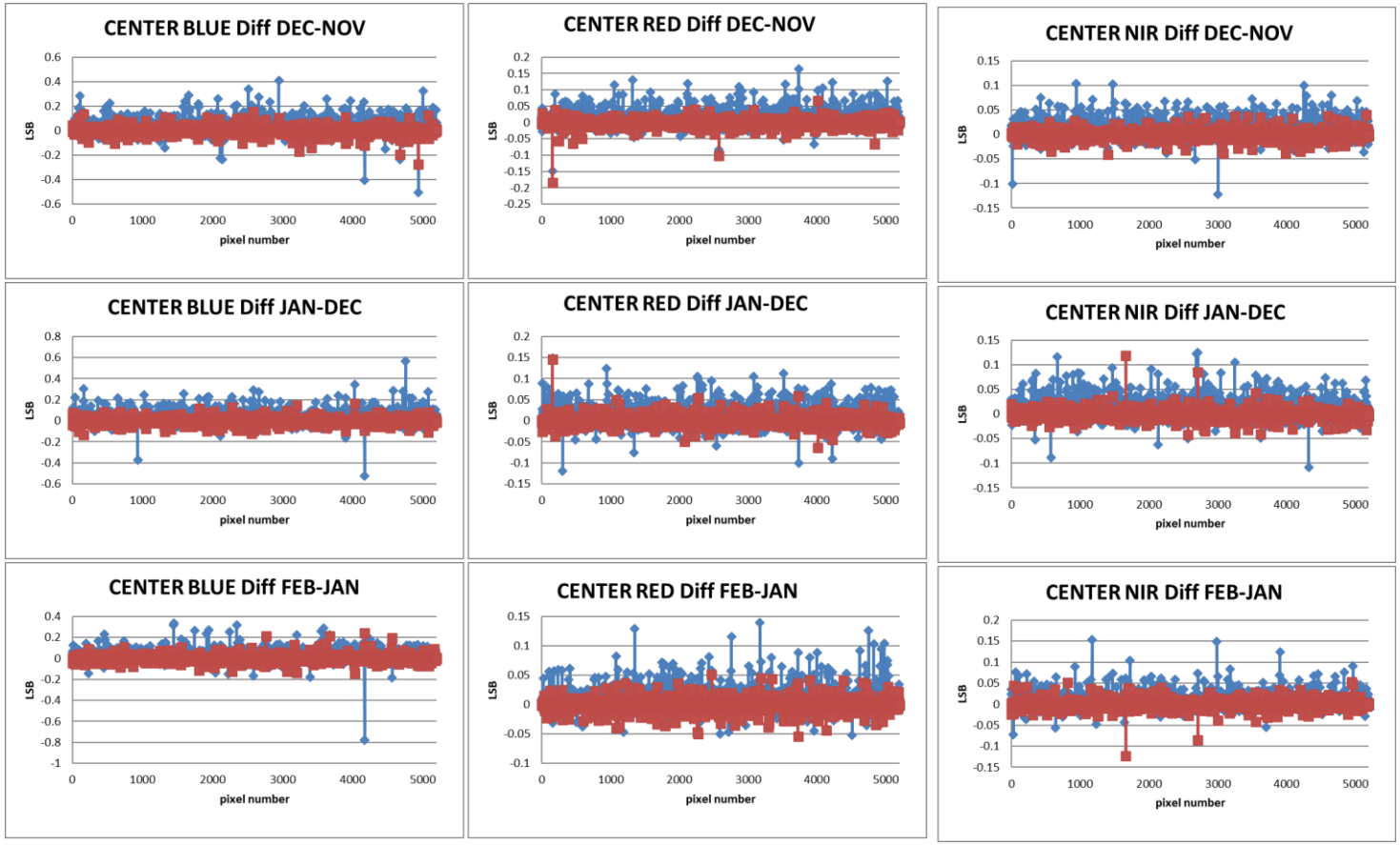

*Figure 13. CENTER camera VNIR: Monthly difference (*NOV 2018-FEB2019*) in dark current (Blue) and standard deviation (Red) of the monthly averaged results.*

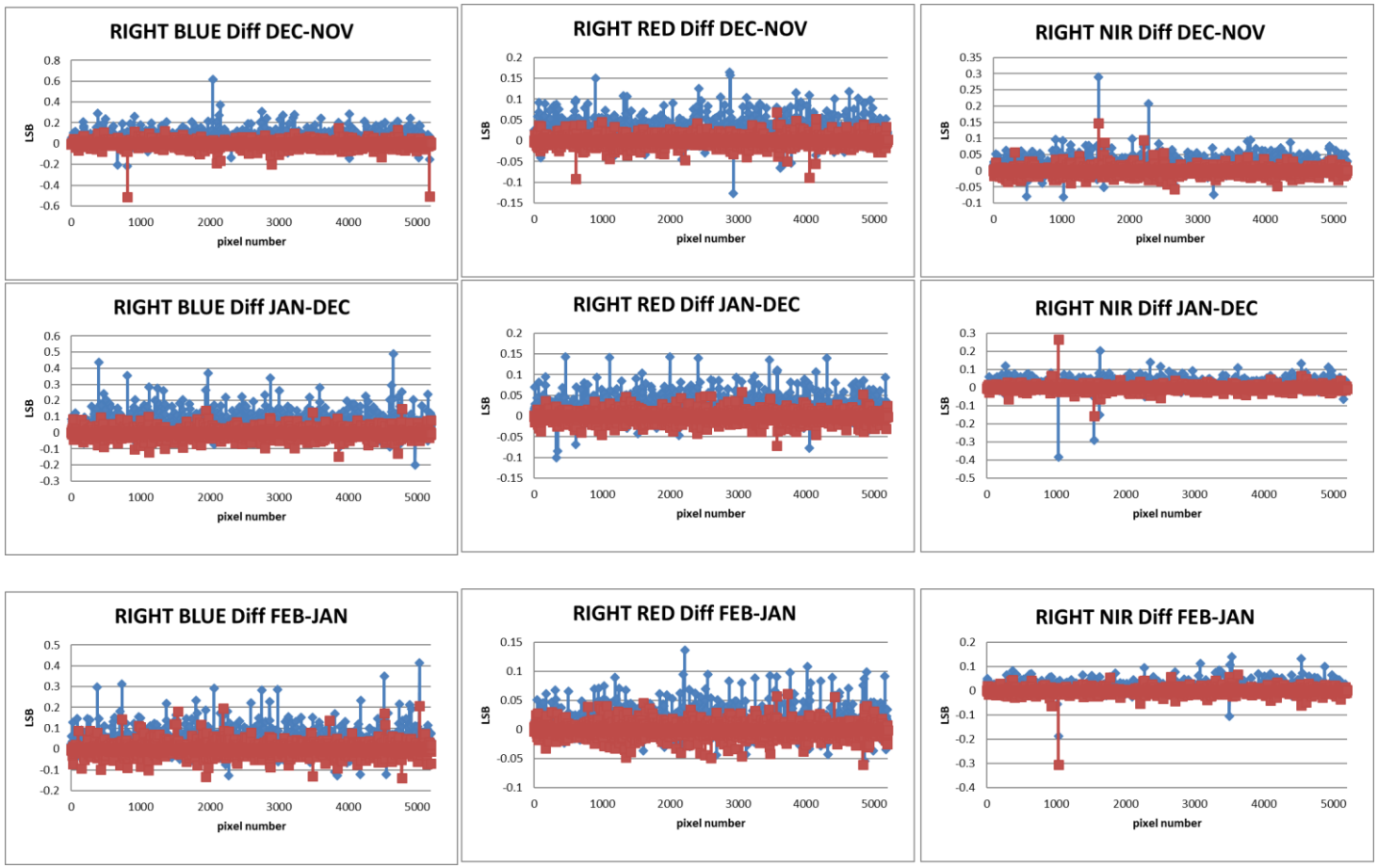

*Figure 14. RIGHT camera VNIR: Monthly difference (*NOV 2018-FEB2019*) in dark current (Blue) and standard deviation (Red) of the monthly averaged results.*

1.3.3. SWIR results

Monthly difference plots for SWIR dark currents are given in Figure 15, Figure 16 and Figure 17 for respectively LEFT, CENTER and RIGHT camera.

A dark current outlier analysis is performed for pixels having for at least one month a dark current expressed in LSB larger than the DC THRESHOLD. This DC THRESHOLD is set to 4 LSB. For those pixels the following dark current pixel statuses are given:

- Both monthly differences > 4 LSB ? **Quality is "H DC BAD"**
- One monthly difference > 4 LSB ? **Quality is "H DC NOK"**.
- Both monthly differences < 4 LSB ? **Quality is "H DC OK"**

In *Table 3* and *Table 5* the resulting SWIR dark current status during the last 3 months is reported for respectively LEFT, CENTER and RIGHT camera.

An increase in the dark currents of the SWIR strips of LEFT and CENTER camera have been observed during last month. This increase might be linked to an increase in the temperature observed during the last weeks.

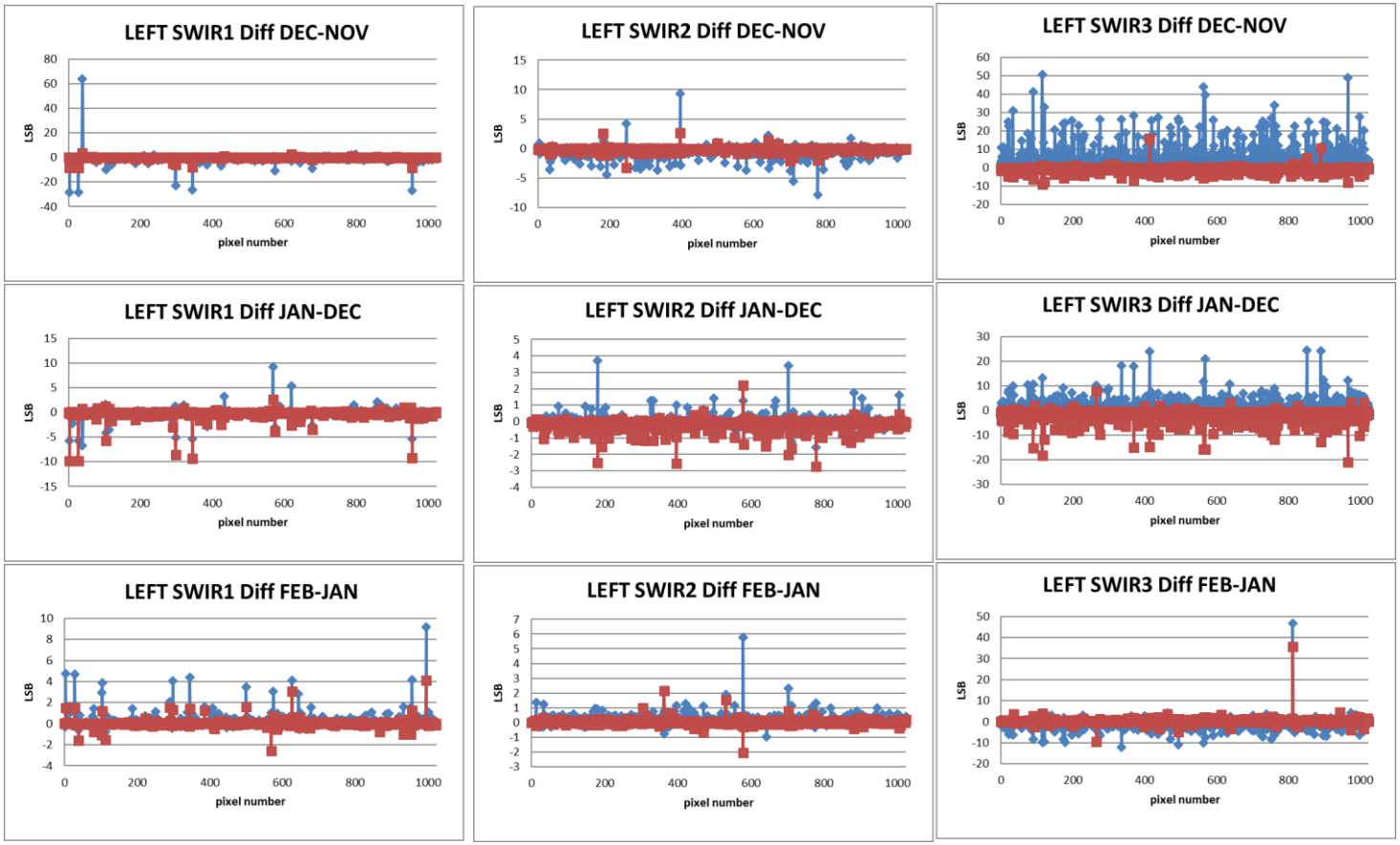

Figure 15. LEFT camera SWIR: Monthly difference (NOV 2018-FEB2019) in dark current (Blue) and standard deviation (Red) of the monthly averaged results.

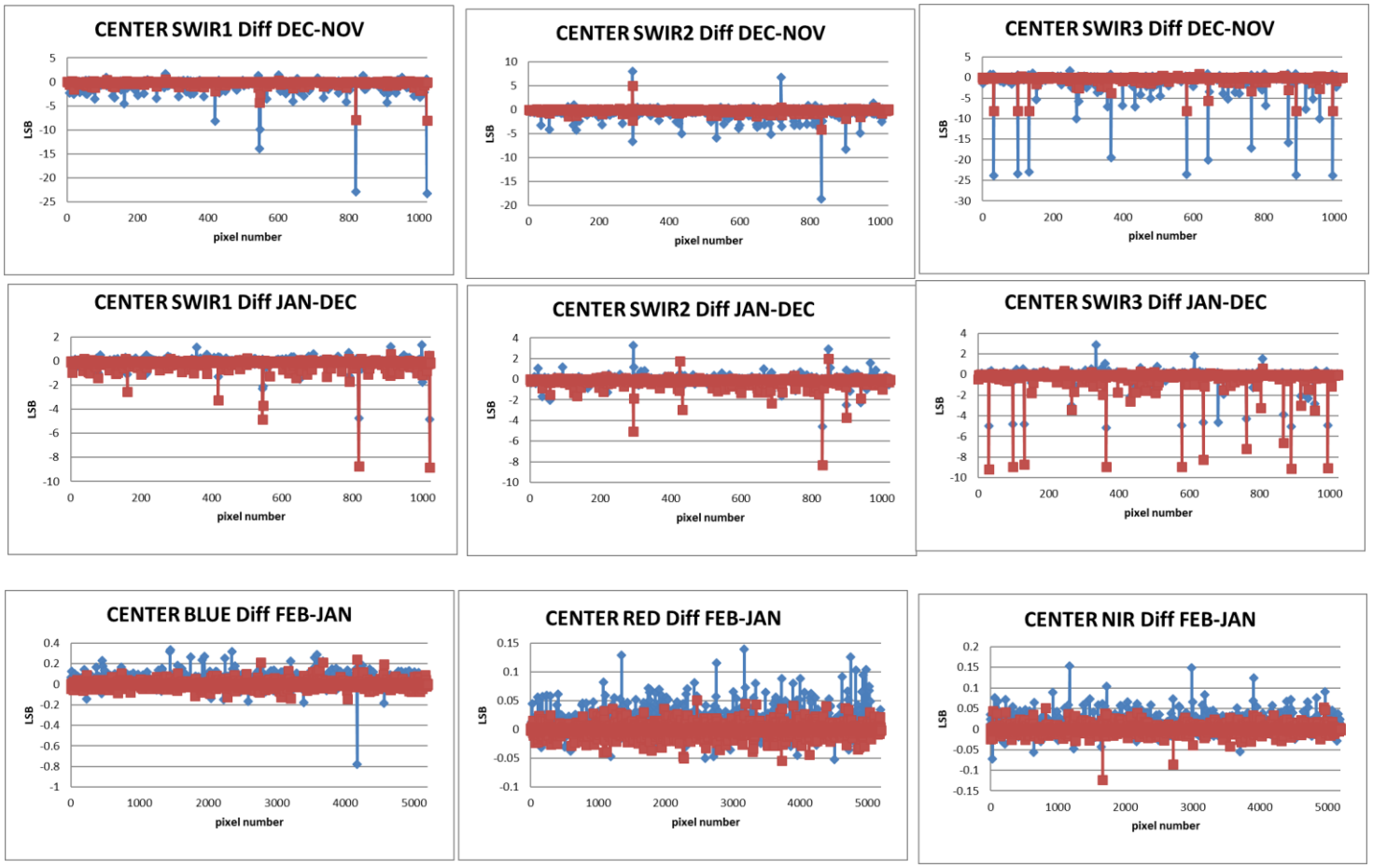

Figure 16. CENTER camera SWIR: Monthly difference (NOV 2018-FEB2019) in dark current (Blue) and standard deviation (Red) of the monthly averaged results.

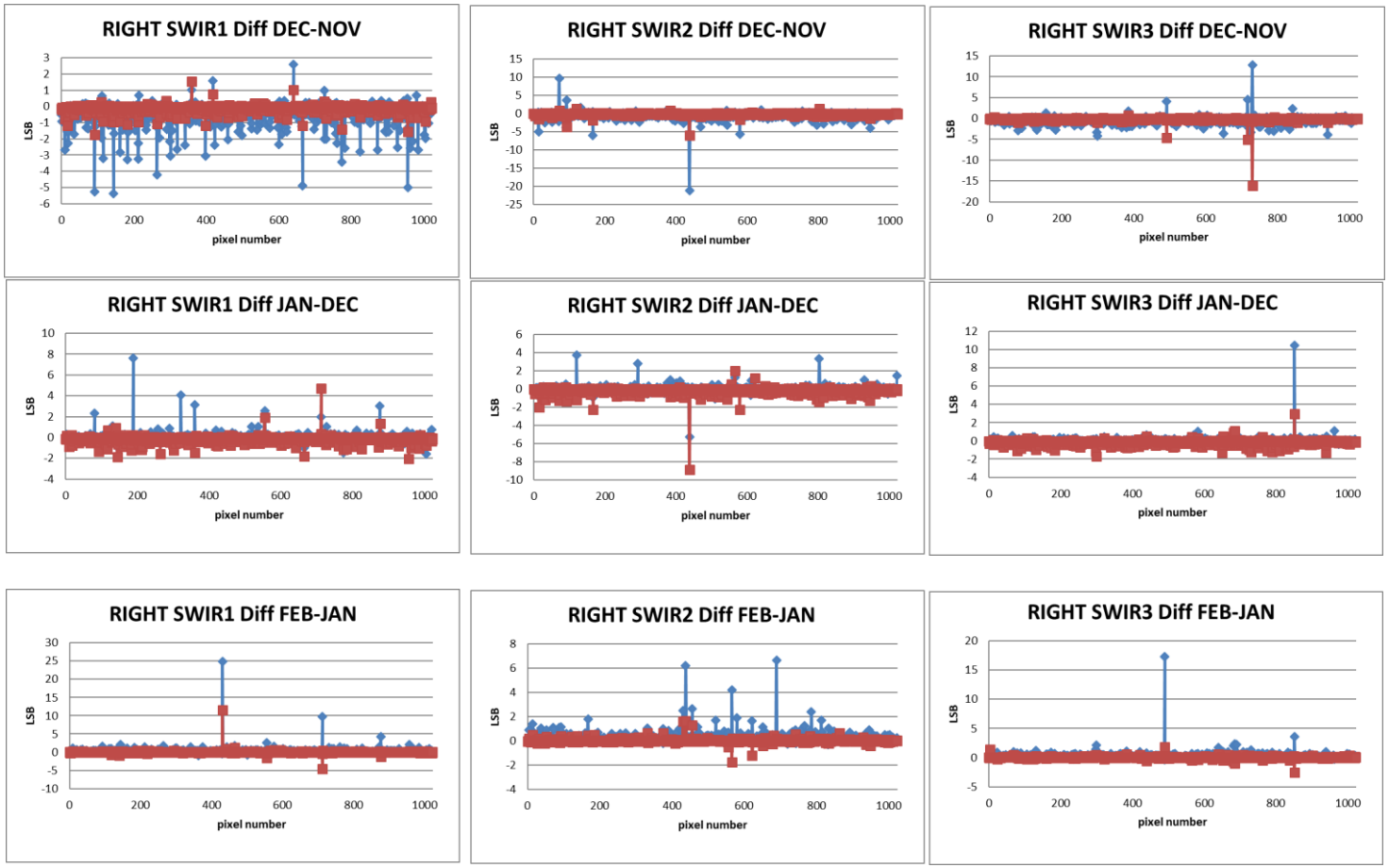

Figure 17. RIGHT camera SWIR: Monthly difference (NOV 2018-FEB2019) in dark current (Blue) and standard deviation (Red) of the monthly averaged results.

LEFT																		
OCT-NOV-DEC						NOV-DEC-JAN						DEC-JAN-FEB						
SWIR1		SWIR2		SWIR3		SWIR1		SWIR2		SWIR3		SWIR1		SWIR2		SWIR3		
3	H DC BAD	711	H DC BAD	201 pixels	H DC BAD	3	H DC BAD	192	H DC BAD	88 pixels	H DC BAD	3	H DC BAD	578	H DC NOK	40 pixels	H DC BAD	
28	H DC BAD	778	H DC BAD	220pixels	H DC NOK	28	H DC BAD	246	H DC BAD	338pixels	H DC NOK	28	H DC BAD	288pixels	H DC OK	67pixels	H DC NOK	
104	H DC BAD	159	H DC NOK	590pixels	H DC OK	39	H DC BAD	396	H DC BAD	589pixels	H DC OK	298	H DC BAD			907pixels	H DC OK	
120	H DC BAD	192	H DC NOK			104	H DC BAD	711	H DC BAD			345	H DC BAD					
187	H DC BAD	246	H DC NOK			298	H DC BAD	778	H DC BAD			956	H DC BAD					
222	H DC BAD	396	H DC NOK			345	H DC BAD	396	H DC NOK			39	H DC BAD					
298	H DC BAD	702	H DC NOK			956	H DC BAD	702	H DC NOK			104	H DC BAD					
345	H DC BAD	922	H DC NOK			120	H DC NOK	922	H DC NOK			569	H DC NOK					
425	H DC BAD	338pixels	H DC OK			187	H DC NOK	314pixels	H DC OK			620	H DC NOK					
575	H DC BAD					222	H DC NOK					626	H DC NOK					
678	H DC BAD					365	H DC NOK					996	H DC NOK					
956	H DC BAD					385	H DC NOK					193pixels	H DC OK					
39	H DC NOK					425	H DC NOK											
78	H DC NOK					569	H DC NOK											
290	H DC NOK					575	H DC NOK											
365	H DC NOK					620	H DC NOK											
385	H DC NOK					644	H DC NOK											
644	H DC NOK					678	H DC NOK											
886	H DC NOK					196pixels	H DC OK											

Table 3. LEFT SWIR dark current pixel outliers (ID L1A).

						CENTER											
OCT-NOV-DEC						NOV-DEC-JAN						DEC-JAN-FEB					
SWIR1		SWIR2		SWIR3		SWIR1		SWIR2		SWIR3		SWIR1		SWIR2		SWIR3	
161	H DC BAD	134	H DC BAD	30	H DC BAD	819	H DC BAD	831	H DC BAD	30	H DC BAD	175	H DC NOK	831	H DC NOK	30	H DC BAD
419	H DC BAD	295	H DC BAD	99	H DC BAD	1021	H DC BAD	57	H DC BAD	99	H DC BAD	819	H DC NOK	236pixels	H DC OK	99	H DC BAD
545	H DC BAD	687	H DC BAD	131	H DC BAD	161	H DC NOK	134	H DC BAD	131	H DC BAD	1021	H DC NOK			131	H DC BAD
547	H DC BAD	831	H DC BAD	152	H DC BAD	419	H DC NOK	294	H DC BAD	364	H DC BAD	199pixels	H DC OK			364	H DC BAD
641	H DC BAD	900	H DC BAD	266	H DC BAD	545	H DC NOK	295	H DC BAD	579	H DC BAD					579	H DC BAD
792	H DC BAD	941	H DC BAD	272	H DC BAD	547	H DC NOK	433	H DC BAD	640	H DC BAD					640	H DC BAD
819	H DC BAD	57	H DC NOK	354	H DC BAD	641	H DC NOK	533	H DC NOK	763	H DC BAD					682	H DC BAD
1021	H DC BAD	294	H DC NOK	364	H DC BAD	792	H DC NOK	687	H DC NOK	890	H DC BAD					763	H DC BAD
18	H DC NOK	433	H DC NOK	397	H DC BAD	908	H DC NOK	716	H DC NOK	994	H DC BAD					890	H DC BAD
77	H DC NOK	533	H DC NOK	432	H DC BAD	211pixels	H DC OK	900	H DC NOK	152	H DC BAD					994	H DC BAD
133	H DC NOK	716	H DC NOK	476	H DC BAD			941	H DC NOK	266	H DC BAD					127pixels	H DC OK
165	H DC NOK	280pixels	H DC OK	504	H DC BAD			244pixels	H DC OK	272	H DC BAD						
908	H DC NOK			579	H DC BAD					354	H DC BAD						
1001	H DC NOK			640	H DC BAD					397	H DC BAD						
230pixels	H DC OK			697	H DC BAD					432	H DC BAD						
				763	H DC BAD					448	H DC BAD						
				804	H DC BAD					476	H DC BAD						
				868	H DC BAD					504	H DC BAD						
				890	H DC BAD					682	H DC BAD						
				917	H DC BAD					697	H DC BAD						
				957	H DC BAD					804	H DC BAD						
				994	H DC BAD					868	H DC BAD						
				448	H DC NOK					917	H DC NOK						
				682	H DC NOK					938	H DC NOK						
				716	H DC NOK					957	H DC NOK						
				729	H DC NOK					126pixels	H DC OK						
				938	H DC NOK												
				1005	H DC NOK												
				135pixels	H DC OK												

Table 4. CENTER SWIR dark current pixel outliers (ID L1A)

RIGHT																	
OCT-NOV-DEC						NOV-DEC-JAN						DEC-JAN-FEB					
92	H DC BAD	14	H DC BAD	300	H DC BAD	92	H DC NOK	438	H DC BAD	300	H DC NOK	189	H DC NOK	438	H DC BAD	490	H DC NOK
144	H DC BAD	167	H DC BAD	492	H DC BAD	144	H DC NOK	14	H DC BAD	492	H DC NOK	321	H DC NOK	566	H DC BAD	852	H DC NOK
264	H DC BAD	438	H DC BAD	717	H DC BAD	189	H DC NOK	72	H DC BAD	717	H DC NOK	431	H DC NOK	689	H DC BAD	284pixels	H DC OK
957	H DC BAD	580	H DC BAD	730	H DC BAD	264	H DC NOK	167	H DC BAD	730	H DC NOK	713	H DC NOK	378pixels	H DC OK		
183	H DC NOK	946	H DC BAD	297	H DC NOK	321	H DC NOK	580	H DC BAD	852	H DC NOK	877	H DC NOK				
459	H DC NOK	72	H DC NOK	939	H DC NOK	666	H DC NOK	946	H DC NOK	299pixels	H DC OK	338pixels	H DC OK				
666	H DC NOK	92	H DC NOK	352pixels	H DC OK	957	H DC NOK	401pixels	H DC OK								
774	H DC NOK	93	H DC NOK			774	H DC NOK										
873	H DC NOK	398	H DC NOK			356pixels	H DC OK										
403pixels	H DC OK	727	H DC NOK														
		460pixels	H DC OK														

Table 5. RIGHT SWIR dark current pixel outliers (ID L1A)

1.4. Yaw manoeuvre: Low Frequency Equalisation

In March 2016 the first yaw-maneuver campaign was executed over the Niger-1 desert zone. During the summer of 2017 and 2018, follow-on campaigns where executed over the same radiometrically uniform desert site.

1.4.1. Method

The first yaw-maneuver calibration campaign was programmed on 11th March 2016. The acquired level 0 data (DN) for all SWIR strips is processed by the PROBA-V Processing Facility up to un-projected level 1C Top Of Atmosphere reflectance, including the pixel-based geo-coordinate annotation. Within the uniform Niger-1 zone, a sub-zone is selected for every SWIR strip. The sub-zone is selected in such way that it allows multiple pixel selection per detector, located within this zone. Based on their geo-location, the un-projected pixels are selected from the image and sorted per detector. After averaging all pixels per detector, a low-pass filter removes the high frequency components form the intermediate PNRU profile. The remaining low frequency profile is then normalized to the mean value of all detector mean reflectance values. This normalized profile is the final profile, used to correct the existing PRU calibration parameters. To gain confidence on the uniformity of the selected Niger-1 sub-zone, the zone itself is split-up in three separate mini-zones. For these mini-zones, again the same image processing procedure is applied. If all resulting mini-zone profiles are identical to the originally derived sub-zone profile, uniformity of the used zone is considered true. After applying this procedure for all 9 strips, it was concluded that the correction is impossible for both off-nadir viewing cameras, with this type of yaw maneuver.
Therefore, in 2017 the yaw campaign was extended with two extra maneuvers for both side cameras. Each time one of the side cameras is pointed towards nadir viewing. This was achieved by 2 successive angular movements of the platform – a 90° yaw combined with approx. 10° roll maneuver (the magnitude of the roll is limited by star-tracker blinding avoidance). To calibrate all 3 cameras, 3 maneuvers have been performed in July and October 2017 . In July 2018, follow-on maneuvers are executed, again separately for all three cameras.

1.4.2. Results

For the CENTER camera, results are presented in Figure 18. The red curve is the characterization of the PRNU (excluding the high frequency component), assessed with the 2016 yaw maneuver. Significant variations can be observed for all three cameras. The results are applied to correct the existing PRNU coefficients in the PROBA-V Radiometric Instrument Calibration files and applied in the nominal processing. The green (2017) and blue (2018) curves are the new yaw results, computed with the nominal parameters.
Figure 19 shows the variation over the SWIR detectors for both left and right cameras for 2017 and 2018 yaw steering data. One can observe quite good agreement between both acquisitions for all strips. The green curve is the application of the derived parameters of 2017 applied to the 2018 yaw results.
The effective reduction in peak to peak variations is tabulated per strip in Table 6. More than 5% reduction can be observed for LEFT and RIGHT SWIR3 strips. LEFT SWIR1, CENTER SWIR3 and RIGHT

SWIR3 clearly have remains of vignetting at the edges of the strips. After correction these effects are removed. Local features are reduced, resulting in increased flatting of the PRU profiles.

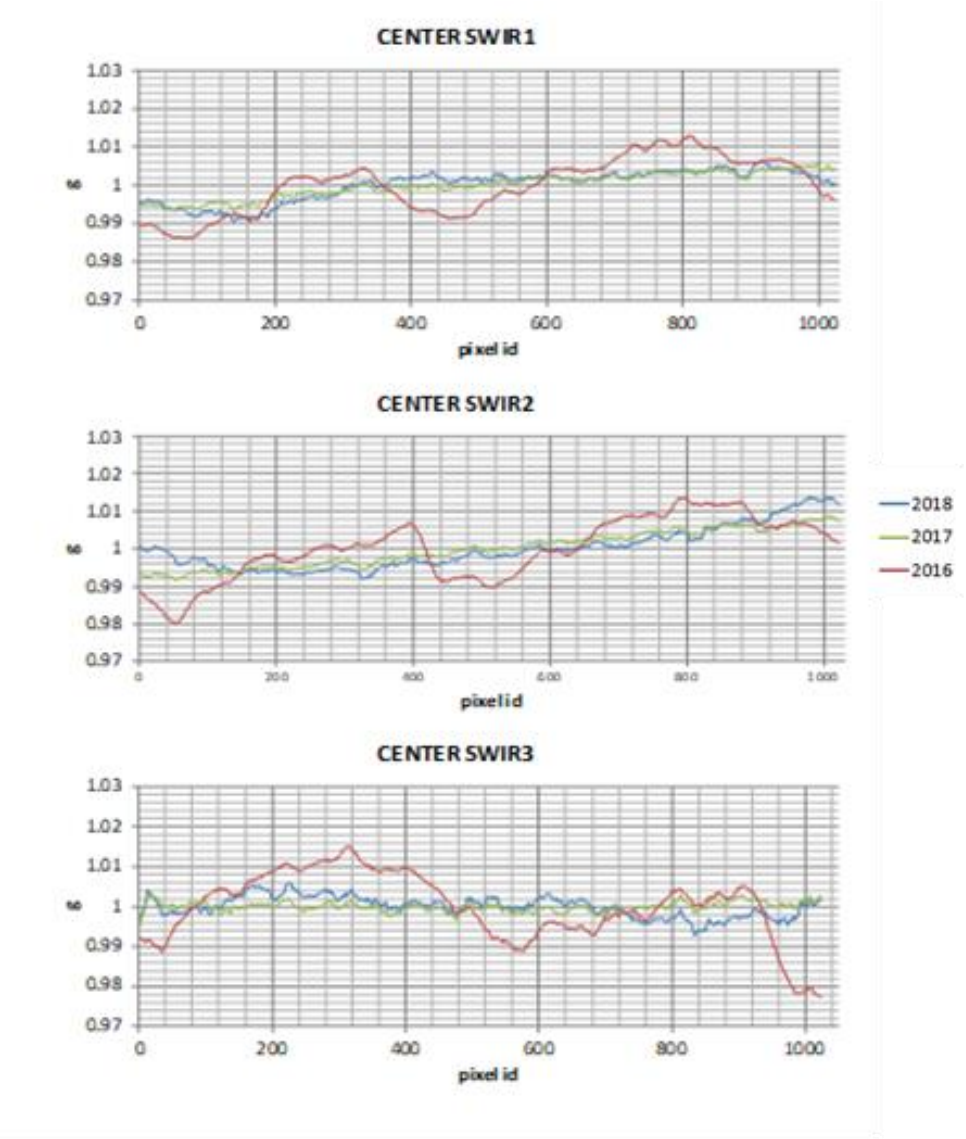

Figure 18 Yaw Results Center Camera

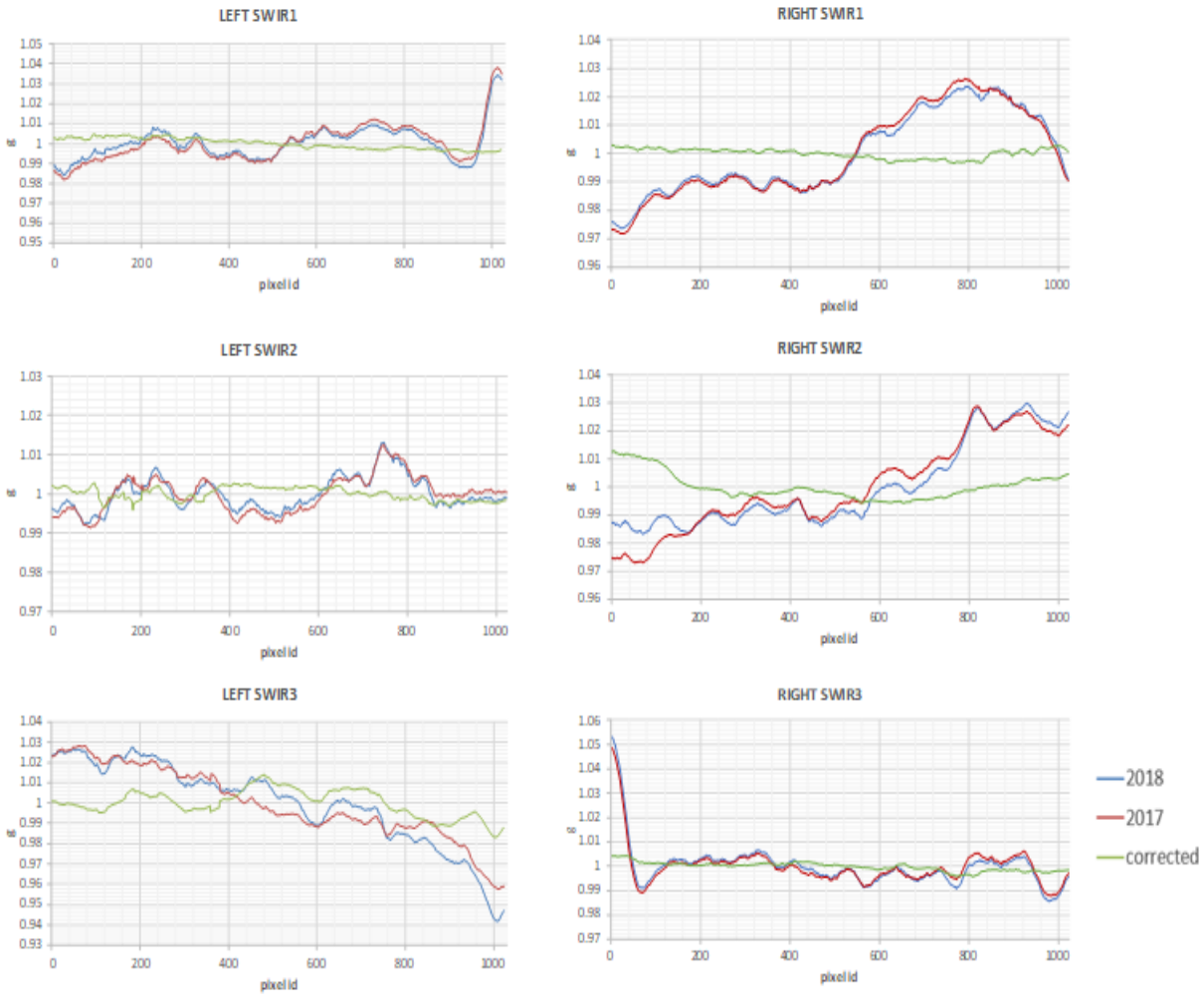

Figure 19 Results for LEFT and RIGHT camera

Table 6. Peak to peak pixel variation per strip and per camera before and after correction

	LEFT		CENTER		RIGHT	
%	**before**	**after**	**before**	**after**	**before**	**after**
SWIR1	5.0547	0.9261	2.6676	1.2539	5.4586	0.6167
SWIR2	2.0814	0.6754	3.3440	1.6354	5.5611	1.8621
SWIR3	8.5838	3.0782	3.7697	0.8014	6.0659	0.8676

1.5. Bad pixels

There is no new bad pixel identified in this reporting period.

Reporting period Mid-Dec 2018- Mid-Mar 2019																
CAMERA	STRIP	pixel numbers (ID L1 A)														
		NEW BAD	BAD (from previous periods)													
left	swir1		3*	28	39	104	298	345	352	644	956					
left	swir2		711	863												
left	swir3		90	172	250	370	419	438	568	759	761					
center	swir1		819	1021												
center	swir2		57	295	769	831	900									
center	swir3		29	30	99	131	448	476	579	640	763	804	889	890	917	938	994
right	swir1															
right	swir2		14	438	470											
right	swir3															

Table 7: Overview Bad pixels

1.6. Radiometric ICP file

The updates to the radiometric ICP file used within the user segment for the processing of the nominal PROBA-V data by PF are listed in the Table 9 for collection 1.

PROBAV_X_R_000_YEARMN01_**101**.xml*	Update dark currents Update of SWIR absolute following linear degradation model**
PROBAV_X_R_000_20161201_01.xml	Update dark currents Update of SWIR absolute following linear degradation model**
PROBAV_X_R_000_20161201_01.xml	Update dark currents Update of SWIR absolute following linear degradation model**
PROBAV_X_R_000_20161201_01.xml	Update dark currents Update of SWIR absolute following linear degradation model**
PROBAV_X_R_000_20161201_01.xml	Update dark currents Update of SWIR absolute following linear degradation model**
PROBAV_X_R_000_20170101_01.xml	Update dark currents Update of SWIR absolute following linear degradation model**
PROBAV_X_R_000_20170120_01.xml	SWIR status map updated : 1 bad pixel added
PROBAV_X_R_000_20170201_01.xml	Update dark currents Update of SWIR absolute following linear degradation model**
PROBAV_X_R_000_20170220_01.xml	SWIR status map updated : 1 bad pixel added

PROBAV_X_R_000_20170301_01.xml	Update dark currents Update of SWIR absolute following linear degradation model**
PROBAV_X_R_000_20170401_01.xml	Update dark currents Update of SWIR absolute following linear degradation model** SWIR status map updated : 1 bad pixel added
PROBAV_X_R_000_2017051_01.xml	Update dark currents Update of SWIR absolute following linear degradation model** Update of LEFT BLUE and CENTER BLUE absolute calibration coefficients following linear degradation model***
PROBAV_X_R_000_20170601_01.xml	Update dark currents Update of SWIR absolute following linear degradation model** Update of LEFT BLUE and CENTER BLUE absolute calibration coefficients following linear degradation model***
PROBAV_X_R_000_20170701_01.xml	Update dark currents Update of SWIR absolute following linear degradation model** Update of LEFT BLUE and CENTER BLUE absolute calibration coefficients following linear degradation model*** SWIR status map updated : 1 bad pixel added
PROBAV_X_R_000_20170801_01.xml	Update dark currents Update of SWIR absolute following linear degradation model** Update of LEFT BLUE and CENTER BLUE absolute calibration coefficients following linear degradation model*** SWIR status map updated : 2 bad pixel added
PROBAV_X_R_000_20170901_01.xml	Update dark currents Update of SWIR absolute following linear degradation model***, new coef applied for RIGHT SWIR strips***** Update of LEFT BLUE and CENTER BLUE absolute calibration coefficients following linear degradation model **with new coef** **** SWIR status map updated : 2 bad pixel added

PROBAV_X_R_000_20171001_01.xml	Update dark currents Update of SWIR absolute following linear degradation model***, new coef applied for RIGHT SWIR strips***** Update of LEFT BLUE and CENTER BLUE absolute calibration coefficients following linear degradation model **with new coef** ****
PROBAV_X_R_000_20171101_01.xml	Update dark currents Update of SWIR absolute following linear degradation model***, new coef applied for RIGHT SWIR strips***** Update of LEFT BLUE and CENTER BLUE absolute calibration coefficients following linear degradation model **with new coef** ****
PROBAV_X_R_000_20171201_01.xml	Update dark currents Update of SWIR absolute following linear degradation model***, new coef applied for RIGHT SWIR strips***** Update of LEFT BLUE and CENTER BLUE absolute calibration coefficients following linear degradation model **with new coef** ****
PROBAV_X_R_000_20180101_01.xml	Update dark currents Update of LEFT and CENTER SWIR absolute following linear degradation model***; **No update of RIGHT SWIR absolute cal**.. Update of LEFT BLUE and CENTER BLUE absolute calibration coefficients following linear degradation model **with new coef** ****
PROBAV_X_R_000_20180201_01.xml	Update dark currents Update of LEFT and CENTER SWIR absolute following linear degradation model***; **No update of RIGHT SWIR absolute cal**.. Update of LEFT BLUE and CENTER BLUE absolute calibration coefficients following linear degradation model **with new coef** ****
PROBAV_X_R_000_20180301_01.xml	Update dark currents Update of LEFT and CENTER SWIR absolute following linear degradation model***; **No update of RIGHT SWIR absolute cal**.. Update of LEFT BLUE and CENTER BLUE absolute calibration coefficients

	following linear degradation model **with new coef** ****
PROBAV_X_R_000_20180401_01.xml	Update dark currents Update of LEFT and CENTER SWIR absolute following linear degradation model***; **No update of RIGHT SWIR absolute cal**.. Update of LEFT BLUE and CENTER BLUE absolute calibration coefficients following linear degradation model **with new coef** ****
PROBAV_X_R_000_20180501_01.xml	Update dark currents Update of LEFT and CENTER SWIR absolute following linear degradation model***; **No update of RIGHT SWIR absolute cal**.. Update of LEFT BLUE and CENTER BLUE absolute calibration coefficients following linear degradation model **with new coef** ****
PROBAV_X_R_000_20180601_01.xml	Update dark currents Update of LEFT and CENTER SWIR absolute following linear degradation model***; **No update of RIGHT SWIR absolute cal**.. Update of LEFT BLUE and CENTER BLUE absolute calibration coefficients following linear degradation model **with new coef** ****
PROBAV_X_R_000_20180701_01.xml	Update dark currents Update of LEFT and CENTER SWIR absolute following linear degradation model***; **No update of RIGHT SWIR absolute cal**.. Update of LEFT BLUE and CENTER BLUE absolute calibration coefficients following linear degradation model **with new coef** ****
PROBAV_X_R_000_20180801_01.xml	Update dark currents Update of LEFT and CENTER SWIR absolute following linear degradation model***; **No update of RIGHT SWIR absolute cal**.. Update of LEFT BLUE and CENTER BLUE absolute calibration coefficients following linear degradation model **with new coef** ****

PROBAV_X_R_000_20180821_01.xml	SWIR status map updated : 1 bad pixel added for SWIR2 center camera + correction for assignment of bad pixel status to wrong pixel ID
PROBAV_X_R_000_20180901_01.xml	Update dark currents Update of LEFT and CENTER SWIR absolute following linear degradation model***; **No update of RIGHT SWIR absolute cal**.. Update of LEFT BLUE and CENTER BLUE absolute calibration coefficients following linear degradation model **with new coef** ****
PROBAV_X_R_000_20181001_01.xml	Update dark currents. Update of LEFT BLUE and CENTER BLUE absolute calibration coefficients following linear degradation model **with new coef** ****
PROBAV_X_R_000_20181101_01.xml	Update dark currents. Update of LEFT BLUE and CENTER BLUE absolute calibration coefficients following linear degradation model **with new coef** ****
PROBAV_X_R_000_20181201_01.xml	Update dark currents. Update of LEFT BLUE and CENTER BLUE absolute calibration coefficients following linear degradation model **with new coef** ****
PROBAV_X_R_000_20190101_01.xml	Update dark currents. Update of LEFT BLUE and CENTER BLUE absolute calibration coefficients following linear degradation model **with new coef** ****
PROBAV_X_R_000_2010201_01.xml	Update dark currents. Update of LEFT BLUE and CENTER BLUE absolute calibration coefficients following linear degradation model **with new coef** ****

PROBAV_X_R_000_20190301_01.xml	Update dark currents. Update of LEFT BLUE and CENTER BLUE absolute calibration coefficients following linear degradation model **with new coef** ****

Table 8: Radiometric ICP-file updates Collection 1

2. Geometric Image Quality

2.1. Summary

The quarterly Average Location Error (ALE) over the period 16/12/2018 – 15/3/2019 was 74 m (1σ = 83 m) for all spectral bands (combined cameras). Compared to the previous reporting period, the ALE has increased (deteriorated) by 4%. The number of chips per day and per spectral band used for the geometric accuracy analysis decreased by 41% on average compared to the previous reporting period, which is mainly caused by the fact that for 13 out of the 90 Q1 days no data were available due to processing issues in the geolocation validation chain.

The daily average location error compliance (ALE < 300m) was 99.23%, which is 0.05% higher than in previous quarter. The inter-band geometric accuracy was 33 – 58 m (standard deviation range is 9 – 16 m), which is 0.10 – 0.17 of a pixel (333 m). The average inter-band RED-NIR registration accuracy was 34 m, which is 1 m lower than in previous reporting period.

The multi-temporal geometric accuracy was 80.98% (28.16% higher compared to previous quarter) for the VNIR and 94.62% (20.62% higher compared to previous quarter) for the combined VNIR/SWIR. The multi-temporal accuracies over the last full year are 75.20% and 89.68% for VNIR and VNIR/SWIR, respectively. The sharp decline in multi-temporal accuracy for Q4 2018 is attributed to the geolocation issue of 19 – 21 September 2018.

The geometric ICP file generated on 8/9/2016, valid from 1/9/2016 has remained valid throughout the reporting period.

2.2. Assessment of the geometric accuracy on L1C data

The absolute location error (ALE) and accompanying standard deviation of the Level1C data is presented in the tables below for each camera, spectral band/strip and reporting month.

CAMERA 1 Mean and standard deviation ALE [m]			
Strip\Period	**16/12/2018 - 15/1/2019**	**16/1/2019 - 15/2/2019**	**16/2/2019 - 15/3/2019**
BLUE	60.25, σ = 36.05	61.62, σ = 35.57	53.07, σ = 30.05
RED	62.12, σ = 38.26	62.81, σ = 37.17	53.12, σ = 30.60
NIR	63.46, σ = 39.65	67.46, σ = 40.16	58.51, σ = 34.48
SWIR1	99.22, σ = 61.63	93.83, σ = 57.78	81.76, σ = 50.81
SWIR2	61.68, σ = 35.36	63.73, σ = 36.44	56.43, σ = 30.93
SWIR3	54.24, σ = 31.92	60.52, σ = 34.70	52.81, σ = 29.53

Table 9: Mean absolute location error and standard deviation (σ) for camera 1.

CAMERA 2 Mean and standard deviation ALE [m]			
Strip\Period	**16/12/2018 - 15/1/2019**	**16/1/2019 - 15/2/2019**	**16/2/2019 - 15/3/2019**
BLUE	65.44, σ = 36.04	65.84, σ = 36.93	54.85, σ = 32.27
RED	65.99, σ = 35.93	65.67, σ = 36.94	53.76, σ = 31.36
NIR	64.64, σ = 35.88	69.68, σ = 39.13	55.37, σ = 32.42
SWIR1	68.06, σ = 36.13	70.30, σ = 37.97	58.73, σ = 34.15
SWIR2	61.96, σ = 36.05	65.65, σ = 38.34	57.00, σ = 34.74
SWIR3	60.22, σ = 37.06	66.72, σ = 40.67	57.94, σ = 35.85

Table 10: Mean absolute location error and standard deviation (σ) for camera 2.

CAMERA 3 Mean and standard deviation ALE [m]			
Strip\Period	**16/12/2018 - 15/1/2019**	**16/1/2019 - 15/2/2019**	**16/2/2019 - 15/3/2019**
BLUE	67.64, σ = 39.01	74.13, σ = 43.61	83.27, σ = 44.63
RED	75.03, σ = 45.53	83.29, σ = 50.62	91.47, σ = 49.83
NIR	69.32, σ = 44.34	76.86, σ = 50.46	85.49, σ = 51.44
SWIR1	69.32, σ = 39.72	74.83, σ = 45.63	75.78, σ = 43.62
SWIR2	73.40, σ = 45.08	81.46, σ = 51.81	87.05, σ = 49.92
SWIR3	100.86, σ = 63.34	111.71, σ = 72.22	119.48, σ = 70.57

Table 11: Mean absolute location error and standard deviation (σ) for camera 3.

In the reporting period the average location error of the Level 1C data was 70.3 m, which is 0.9 m (1.3%) higher than in the previous quarter.

2.3. Assessment of the geometric accuracy on L2 data

2.3.1. Absolute geometric accuracy

The daily summary of the L2 data absolute location error for all spectral bands is presented in the tables and figures below for the three reporting months:

- from 16/12/2018 – 15/1/2019
- from 16/1/2019 – 15/2/2019
- from 16/2/2019 – 15/3/2019

The tables list:

- The day of the measurement in format dd-mm-yy
- The daily achieved compliance (%B) for the BLUE band (% of GCP where ALE <=300m)
- The daily achieved compliance (%R) for the RED band (% of GCP where ALE <=300m)
- The daily achieved compliance (%N) for the NIR band (% of GCP where ALE <=300m)
- The daily achieved compliance (%S) for the SWIR band (% of GCP where ALE <=450m)

- The number of GCP per day (NB-B) used to derive the absolute location error ALE for the BLUE band
- The daily average ALE (in m) for the BLUE band (MU-B)
- The daily ALE standard deviation (in m) for the BLUE band (STD-B)

- The number of GCP per day (NB-R) used to derive the absolute location error ALE for the RED band
- The daily average ALE (in m) for the RED band (MU-R)
- The daily ALE standard deviation (in m) for the RED band (STD-R)

- The number of GCP per day (NB-N) used to derive the absolute location error ALE for the NIR band
- The daily average ALE (in m) for the NIR band (MU-N)
- The daily ALE standard deviation (in m) for the NIR band (STD-N)

- The number of GCP per day (NB-S) used to derive the absolute location error ALE for the SWIR band
- The daily average ALE (in m) for the SWIR band (MU-S)
- The daily ALE standard deviation (in m) for the SWIR band (STD-S)

Day	%B	%R	%N	%S	NB-B	MU-B	STD-B	NB-R	MU-R	STD-R	NB-N	MU-N	STD-N	NB-S	MU-S	STD-S
16/12/2018	98.75	99.21	99.09	99.67	26911	74.87	96.28	29341	66.24	80.55	29198	65.61	83.79	27602	71.35	80.62
17/12/2018	98.91	99.32	99.34	99.77	30050	69.74	89.05	32622	62.27	68	32034	60.37	67.17	29366	66.51	71.99
18/12/2018	99.12	99.57	99.59	99.78	28028	69.15	89.36	31018	61.17	70.6	29917	58.28	65.68	28993	66.86	78.45
19/12/2018	99.03	99.6	99.47	99.67	26652	68.84	82.82	29892	61.86	64.76	29161	60.42	77.99	29281	68.36	85.78
20/12/2018	98.8	99.36	99.38	99.69	26711	71.47	90.9	29222	63.91	74.44	27569	62.36	69.61	28121	69.27	89.09
21/12/2018	98.89	99.41	99.45	99.76	28927	68.83	84.63	32042	61.01	69.09	30121	60.19	70.66	29589	65.05	73.75
22/12/2018	99.18	99.57	99.59	99.81	29219	64.33	81.05	32906	57.14	68.64	31274	56.49	61.66	30781	62.44	68.17
23/12/2018	98.71	99.52	99.52	99.75	25746	71.56	98.02	30425	61.05	69.68	29345	59.76	75.89	29745	66.55	86.14
24/12/2018	98.36	99.27	99.22	99.73	21837	73.39	102.38	25553	62.56	75.89	25117	62.65	83.25	24841	65.34	77.99
25/12/2018	NoData	NoData	NoData	NoData	NoData	NoData	NoData	NoData	NoData	NoData	NoData	NoData	NoData	NoData	NoData	NoData
26/12/2018	98.76	98.93	98.76	100	726	87.44	82.35	838	90.12	64.85	725	98.62	77.08	855	84.32	53.78
27/12/2018	98.88	99.59	99.47	99.73	23085	78.31	100.03	26604	67.78	71.14	26343	64.46	76.18	25429	73.37	81.04
28/12/2018	98.45	99.22	99.32	99.65	22487	84.02	94.79	25793	75.57	80.58	26326	70.84	74.59	25209	80.9	89.64
29/12/2018	98.27	98.85	99.07	99.62	21967	90.6	106.43	24599	81.2	94.63	24803	77.03	79.14	23709	86.08	93.24
30/12/2018	98.36	99.16	99.13	99.67	25261	87.87	95.53	27888	77.19	72.81	28238	73.91	76.51	24950	84.31	77.49
31/12/2018	98.81	99.26	99.32	99.76	21764	84.71	84.84	24514	75.86	76.9	24546	69.88	69.59	22151	82.5	78.34
01/01/2019	98.36	99.18	99.35	99.71	20296	88.23	99.98	24167	76.22	80.41	23740	71.47	95.25	23396	82.27	88.89
02/01/2019	98.01	98.99	99.14	99.67	21612	84.57	113.37	24845	74.77	88.03	24440	71.54	87.49	23759	78.96	85.7
03/01/2019	98.32	99.1	99.13	99.6	23030	81.88	115.23	25660	72.61	78.19	25203	70.9	83.46	24912	78.47	93.53
04/01/2019	98.67	99.42	99.51	99.76	27409	74.49	97.66	30482	66.58	70.96	30484	64.23	67	28503	72.53	79.46
05/01/2019	98.84	99.49	99.58	99.78	19489	69.7	87.21	22931	62.51	72.46	22853	59.84	63.96	22375	67.62	78.64
06/01/2019	98.76	99.41	99.38	99.73	19161	73.1	106.06	23170	64.33	79.31	23456	62.13	87.47	23232	68.21	78.24
07/01/2019	98.52	99.19	99.31	99.63	19874	80.03	105.14	22851	70.93	78.86	22685	69.45	76.89	21809	77.07	92.14
08/01/2019	98.5	99.16	98.96	99.68	21014	84.75	99.79	23552	75.03	78.2	23488	74.88	93.48	21810	81.17	84.63
09/01/2019	98.62	99.18	99.35	99.76	20891	84.31	93.38	23197	76.64	78.6	23660	71.45	71.86	21820	81.32	82.31
10/01/2019	98.92	99.4	99.49	99.72	22626	75.81	99.62	25737	67.28	79.95	25818	63.88	81.41	24338	72.18	80.91
11/01/2019	98.68	99.33	99.36	99.7	22889	76.1	110.9	26083	65.94	92.13	26035	62.67	82.39	25743	69.35	75.86
12/01/2019	98.69	99.31	99.39	99.69	28501	77.35	105.46	31500	67.59	71.99	30790	64.63	72.1	30251	73.87	84.78
13/01/2019	98.3	99.02	99.27	99.7	24289	92.64	104.29	26435	81.97	83	26991	74.87	74.66	25085	85.39	76.45
14/01/2019	97.94	98.74	98.97	99.7	21246	120.12	103.97	23307	109.04	89.66	24382	100.37	84.51	22306	110.58	86.82
15/01/2019	98.01	98.69	98.98	99.63	20249	113.37	100.45	23389	102.64	96.2	23706	93.93	78.98	22710	107.5	92.61
Averages	**98.61**	**99.25**	**99.3**	**99.72**	**23956**	**80.72**	**97.37**	**25179**	**71.97**	**77.35**	**24917**	**69.24**	**76.99**	**22320**	**76.66**	**81.55**

Table 12: Daily achieved compliance and the daily average location error (in m) for all spectral bands in the period 16/12/2018 – 15/1/2019.

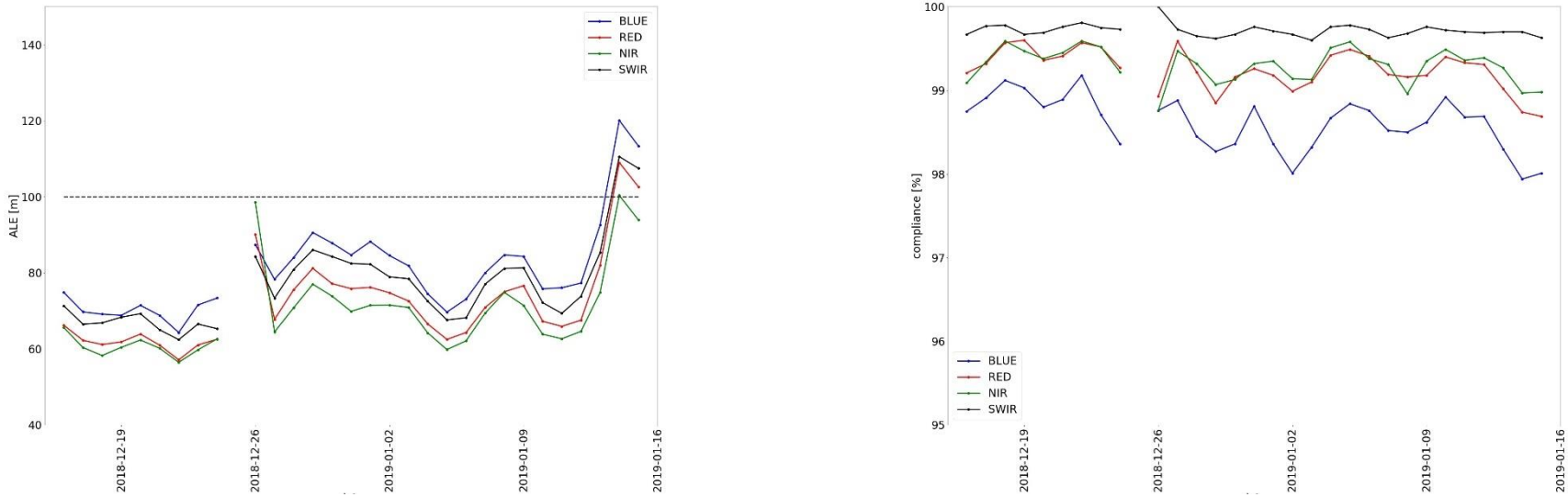

Figure 20: Daily average location error in the period from 16/12/2018 – 15/1/2019 (left) and the average daily compliance of the spectral bands (right).

The root cause of the geolocation issue of 19 – 21 September 2019 that was reported in previous QIR, was found by Qinetiq being due to noisy GPS data, which could only be fixed by a GPS power cycle.

Day	%B	%R	%N	%S	NB-B	MU-B	STD-B	NB-R	MU-R	STD-R	NB-N	MU-N	STD-N	NB-S	MU-S	STD-S
16/01/2019	97.52	98.48	98.74	99.6	22772	115.22	108.2	25372	102.77	88.49	25743	97.29	83.68	24729	106.64	93.42
17/01/2019	98.2	99	99.16	99.7	25480	100.9	104.51	27751	90.52	87.66	27401	84.09	82.93	26008	95.37	83.99
18/01/2019	99.03	99.46	99.55	99.73	23878	78.14	84.48	28054	69.74	68.72	27854	64.73	72.83	26321	76.72	76.63
19/01/2019	98.32	99.37	99.31	99.72	19568	74.14	103.35	22729	63.74	73.35	22058	62.3	71.59	22401	69.38	87.4
20/01/2019	97.9	98.87	99.04	99.71	21635	81.63	106.51	24513	73.46	85.04	24467	71.99	83	25109	71.79	83.46
21/01/2019	98.33	99.22	99.3	99.74	27613	76.58	100.12	30922	68.53	78.58	29945	69.89	78.9	30328	70.29	78.38
22/01/2019	98.77	99.34	99.43	99.77	27900	73.65	96.98	30985	66.14	78.73	30062	64.79	78.55	28636	70.18	74.88
23/01/2019	99	99.51	99.52	99.8	25727	76.83	88.21	28533	69.87	73.71	26757	66.78	71.89	26092	73.54	74.18
24/01/2019	98.99	99.42	99.41	99.74	24824	77.54	93.72	28117	70.01	78.24	27241	66	80.65	27278	74.2	84.45
25/01/2019	98.56	99.31	99.28	99.69	25424	74.62	97.18	27813	65.45	79.5	26790	64.23	80.26	27571	69.33	82.58
26/01/2019	98.93	99.4	99.31	99.7	25699	71.95	86.82	28810	64.01	77.7	28381	61.68	75.14	27214	67.65	78.22
27/01/2019	98.95	99.47	99.48	99.81	20995	74.26	91.48	25202	66.91	65.03	24774	64.55	63.56	23935	68.33	63.15
28/01/2019	98.9	99.51	99.53	99.74	21299	73.22	86.9	24820	65.14	70.06	25075	62.16	69.02	24203	69.32	75.22
29/01/2019	98.52	99.27	99.25	99.71	21343	72.04	94.92	25062	63.57	74.19	25142	62.24	81.1	24285	66.43	80.87
30/01/2019	98.58	99.25	99.23	99.62	25644	77.27	91.85	28276	69.74	81.33	27329	68.59	74.1	26383	70.99	85.27
31/01/2019	98.8	99.38	99.4	99.69	26863	73.49	89.4	29987	65.75	72.27	29266	63.86	70.51	27861	70.27	86.09
01/02/2019	99.17	99.52	99.57	99.74	26703	69.87	87.41	30201	62.88	71.3	29712	60.49	67.3	28199	67.09	78.62
02/02/2019	98.53	99.37	99.36	99.69	22361	75.32	102.37	25881	66.51	86.6	26054	64.95	76.98	25076	68.01	88.12
03/02/2019	98.75	99.25	99.26	99.71	23858	74.26	101.45	27240	66.38	79.53	27301	65.57	72.15	26796	68.08	82.5
04/02/2019	98.73	99.28	99.38	99.72	26091	74.63	99.64	27533	67.52	77.26	27577	65.12	70.13	26820	68.99	77.09
05/02/2019	98.83	99.44	99.37	99.74	25688	69.17	85.47	28820	62.76	74.49	27995	63.49	74.17	26865	66.08	72.85
06/02/2019	98.51	99.28	99.4	99.75	22479	72.95	89.38	25951	65.92	80.93	25747	65.41	80.56	25338	69.81	77.86
07/02/2019	98.53	99.17	99.32	99.73	24748	73.77	99.68	27638	66.16	85.41	27646	63.34	79.33	27427	68.78	84.93
08/02/2019	98.59	99.26	99.39	99.66	27812	73.55	103.12	28982	64.37	75.6	27711	62.29	71.42	26344	68.04	84.15
09/02/2019	98.71	99.3	99.31	99.7	25795	79.37	90.88	27593	70.85	72.25	26840	68.42	79.98	24285	74.72	78.73

10/02/2019	98.86	99.33	99.31	99.79	24898	75.86	94.88	27062	68.96	83.52	26444	67.01	74.9	24831	71.4	68.72
11/02/2019	98.67	99.31	99.3	99.68	21386	75.99	97.94	25372	68.36	78.49	24907	66.9	81.95	24842	71.3	84.25
12/02/2019	98.35	99.28	99.3	99.75	5225	91.2	94.53	5142	75.09	70.21	4708	75.34	80.88	5697	76.83	70.89
13/02/2019	NoData	NoData	NoData	NoData	NoData	NoData	NoData	NoData	NoData	NoData	NoData	NoData	NoData	NoData	NoData	NoData
14/02/2019	NoData	NoData	NoData	NoData	NoData	NoData	NoData	NoData	NoData	NoData	NoData	NoData	NoData	NoData	NoData	NoData
15/02/2019	98.65	99.32	99.38	99.73	12701	89.57	102.52	13976	79.37	75.16	14107	75.16	69.5	14075	82.92	76.87
Averages	**98.63**	**99.29**	**99.33**	**99.72**	**21819**	**78.17**	**95.65**	**24462**	**69.67**	**77.36**	**24033**	**67.54**	**75.76**	**23385**	**72.84**	**79.79**

Table 13: Daily achieved compliance and the daily average location error (in m) for all spectral bands in the period 16/1/2019 – 15/2/2019.

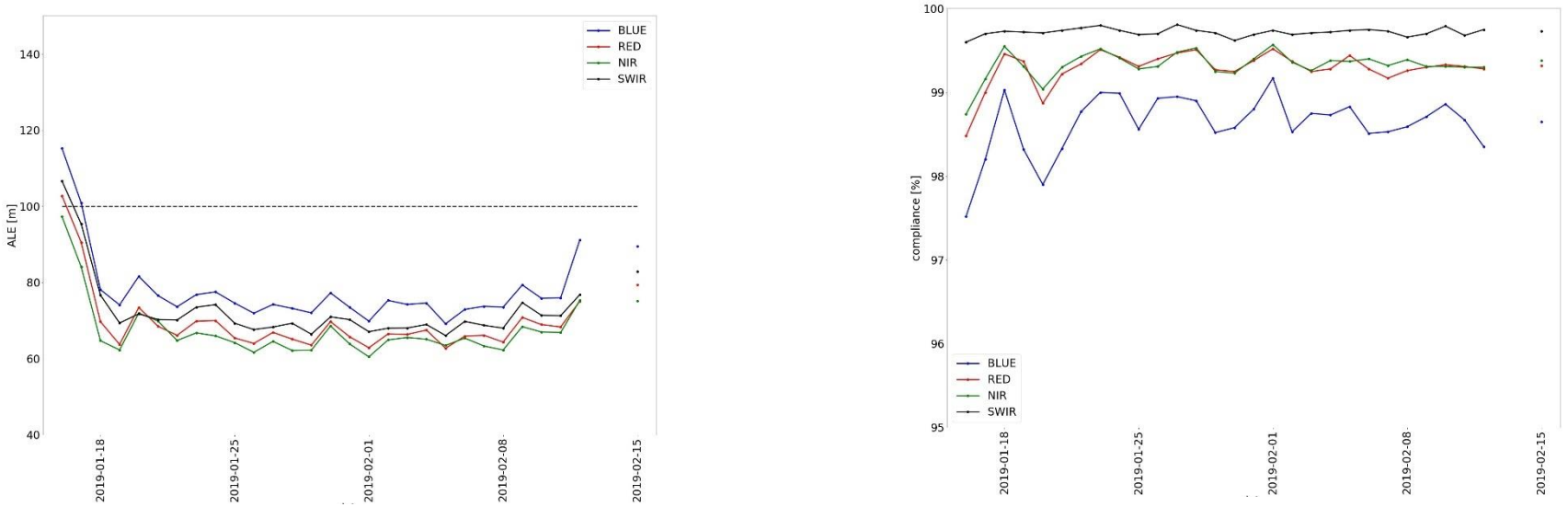

Figure 21: Daily average location error in the period from 16/1/2019 – 15/2/2019 (left) and the average daily compliance of all spectral bands (right).

Day	%B	%R	%N	%S	NB-B	MU-B	STD-B	NB-R	MU-R	STD-R	NB-N	MU-N	STD-N	NB-S	MU-S	STD-S
16/02/2019	NoData	NoData	NoData	NoData	NoData	NoData	NoData	NoData	NoData	NoData	NoData	NoData	NoData	NoData	NoData	NoData
17/02/2019	98.1	98.61	98.83	99.51	11922	107.67	114.68	13539	98.69	89.57	13619	93.86	91.4	12962	101.97	92.09
18/02/2019	99.19	99.45	99.34	99.81	7069	74.57	74.52	8440	69.64	62.57	8233	66.72	71.67	4677	71.01	79.19
19/02/2019	99.23	99.49	99.5	99.76	5183	73.55	71.22	5135	65.73	67.3	4810	64.21	79.3	5716	69.92	70.29
20/02/2019	98.68	99.19	99.24	99.7	11700	82.8	94.85	13999	74.88	85.75	14187	70.02	67.6	13926	77.46	86.47
21/02/2019	NoData	NoData	NoData	NoData	NoData	NoData	NoData	NoData	NoData	NoData	NoData	NoData	NoData	NoData	NoData	NoData
22/02/2019	98.45	99.15	99.24	99.75	16612	75.45	94.11	18622	67.55	74	18071	63.99	74.14	16526	71.88	75.57
23/02/2019	NoData	NoData	NoData	NoData	NoData	NoData	NoData	NoData	NoData	NoData	NoData	NoData	NoData	NoData	NoData	NoData
24/02/2019	99.1	99.31	99.41	99.68	17157	71.05	85.38	18935	65.74	69.86	19018	60.92	66.57	16796	74.09	93.69
25/02/2019	NoData	NoData	NoData	NoData	NoData	NoData	NoData	NoData	NoData	NoData	NoData	NoData	NoData	NoData	NoData	NoData
26/02/2019	98.16	98.9	98.81	99.53	13885	96.49	110.24	15662	87.67	86.22	15266	84.42	89.56	15344	93.21	95.99
27/02/2019	98.37	99.04	99.23	99.73	14321	84.67	98.05	16820	79.98	81.96	16264	75.62	73.61	15733	85.66	87.65
28/02/2019	NoData	NoData	NoData	NoData	NoData	NoData	NoData	NoData	NoData	NoData	NoData	NoData	NoData	NoData	NoData	NoData
01/03/2019	98.68	99.08	99.22	99.73	21391	86.39	103.21	24807	80.94	89.64	24609	77.32	73.96	24575	81.83	89.57
02/03/2019	98.36	99.16	99	99.66	22828	83.66	101.52	24705	76.72	82.72	24624	74.51	85.07	24071	76.1	90.02
03/03/2019	98.96	99.27	99.3	99.73	29222	75.54	85.14	32365	70.94	80.76	30535	68.39	83.15	29747	69.34	81.22
04/03/2019	98.88	99.25	99.29	99.78	10332	73.99	78.27	10792	72.21	79.11	10617	68.2	76.47	8160	72.04	71.5
05/03/2019	98.9	99.11	99.26	99.76	11653	80.91	92.14	12783	77.26	89.31	13144	73.17	84.91	10535	74.48	79.71
06/03/2019	98.96	99.29	99.29	99.74	12651	74.18	90.98	13686	69.39	75.01	13633	68.01	78.84	8512	75.5	83.32
07/03/2019	97.89	98.99	99.17	99.6	5453	70.58	103.71	5949	65.64	78.67	6027	64.03	65.55	4521	67.08	103.54
08/03/2019	98.59	99.34	99.3	99.78	9648	86.57	97.1	11264	77.16	82.09	11492	70.53	66.68	10773	75.17	87.09
09/03/2019	99.37	99.5	99.45	99.79	15083	68.63	75.03	16679	63.84	73.88	16129	61.43	68.25	9659	68.16	74.87
10/03/2019	98.92	99.18	99	99.6	9540	77.14	93.33	9927	77.53	90.84	7987	77.64	88.08	7793	81.16	81.6
11/03/2019	NoData	NoData	NoData	NoData	NoData	NoData	NoData	NoData	NoData	NoData	NoData	NoData	NoData	NoData	NoData	NoData
12/03/2019	NoData	NoData	NoData	NoData	NoData	NoData	NoData	NoData	NoData	NoData	NoData	NoData	NoData	NoData	NoData	NoData
13/03/2019	NoData	NoData	NoData	NoData	NoData	NoData	NoData	NoData	NoData	NoData	NoData	NoData	NoData	NoData	NoData	NoData
14/03/2019	NoData	NoData	NoData	NoData	NoData	NoData	NoData	NoData	NoData	NoData	NoData	NoData	NoData	NoData	NoData	NoData
15/03/2019	NoData	NoData	NoData	NoData	NoData	NoData	NoData	NoData	NoData	NoData	NoData	NoData	NoData	NoData	NoData	NoData
Averages	**98.75**	**99.2**	**99.27**	**99.71**	**11872**	**82.14**	**92.44**	**13363**	**75.12**	**77.63**	**13021**	**71.72**	**75.72**	**12126**	**77.12**	**82.83**

Table 14: Daily achieved compliance and the daily average location error (in m) for all spectral bands in the period 16/2/2019 – 15/3/2019.

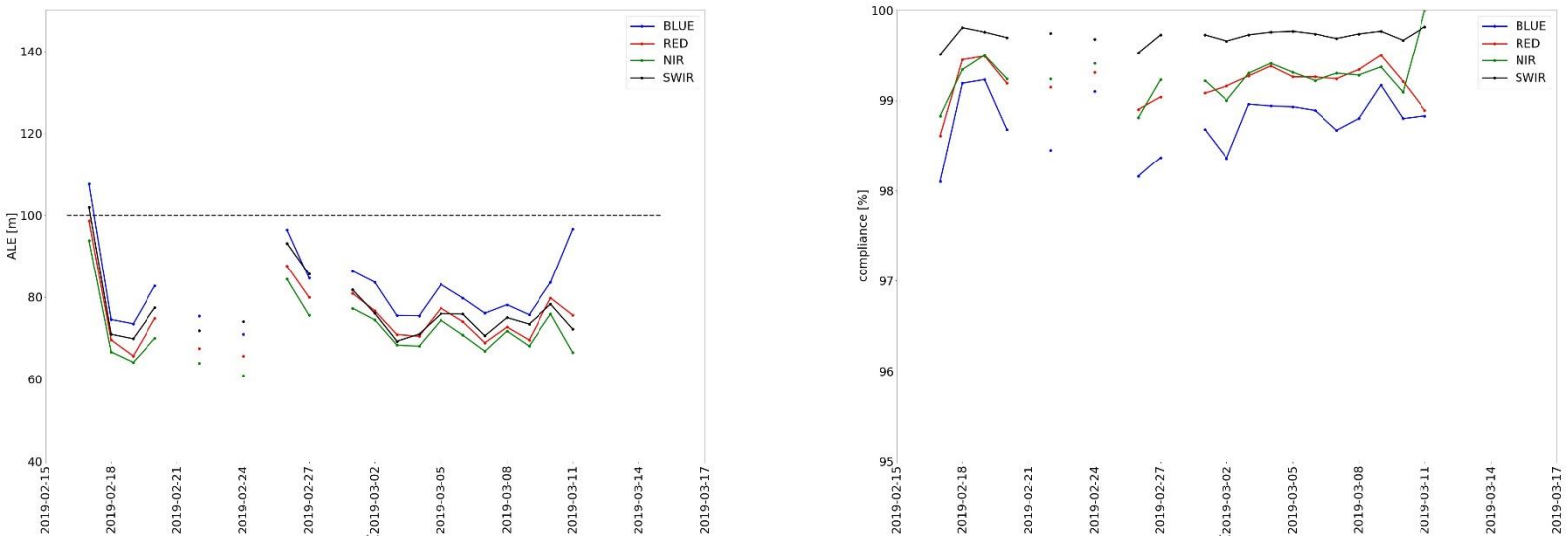

Figure 22: Daily average location error in the period from 16/2/2019 – 15/3/2019 (left) and the average daily compliance of all spectral bands (right).

2.3.2. Inter-band geometric accuracy

The monthly average inter-band geolocation error for all spectral band combinations was as follows:

Band pair	Inter-band error [m]
BLUE-RED	35.34, σ = 9.07
BLUE-NIR	51.95, σ = 16.40
BLUE-SWIR	55.31, σ = 13.05
RED-NIR	34.52, σ = 16.49
RED-SWIR	44.56, σ = 9.33
NIR-SWIR	45.10, σ = 8.51

Table 15: Inter-band geolocation accuracy for period 16/12/2018 – 15/1/2019 for the combined cameras, at 95% confidence level.

Band pair	Inter-band error [m]
BLUE-RED	35.17, σ = 8.88
BLUE-NIR	51.82, σ = 16.11
BLUE-SWIR	55.80, σ = 13.64
RED-NIR	33.05, σ = 13.75
RED-SWIR	45.92, σ = 9.02
NIR-SWIR	47.24, σ = 8.66

Table 16: Inter-band geolocation accuracy for period 16/1/2019 – 15/2/2019 for the combined cameras, at 95% confidence level.

Band pair	Inter-band error [m]
BLUE-RED	37.82, σ = 10.27
BLUE-NIR	54.27, σ = 18.33
BLUE-SWIR	57.84, σ = 14.94
RED-NIR	33.17, σ = 14.75
RED-SWIR	46.53, σ = 9.59
NIR-SWIR	47.21, σ = 9.02

Table 17: Inter-band geolocation accuracy for period 16/2/2019 – 15/3/2019 for the combined cameras, at 95% confidence level.

For the combined cameras, the inter-band geometric accuracy range was 33 – 58 m (standard deviation range is 9 – 16 m), which is 0.10 – 0.17 of a pixel (333 m). The average inter-band RED-NIR registration accuracy was 34 m, which is 1 m lower than previous reporting period.

2.3.3. Multi-temporal geometric accuracy

During this reporting period the multi-temporal compliance of the geometric accuracy was:

- 80.98% for the VNIR sensor (117656 GCPs used),
- 94.62% for the VNIR/SWIR combined (130734 GCPs used).

The multi-temporal sensor compliance has increased by 28.16% for the VNIR sensor and increased by 20.62% for the combined VNIR/SWIR sensors as compared to the previous reporting period (in which values were 52.82% and 74.00%, respectively). The current values correspond again with those of Q3 2018 and before. The anomalous values that were reported for Q4 2018 were influenced by the geolocation issue of 19 – 21 September 2018. This is confirmed by the compliance values calculated over the period 22 September – 21 December, i.e., starting after the geolocation issue. For this period, the compliance values are 83.37% and 95.07% for VNIR and VNIR/SWIR combined, respectively.

For the VNIR the multi-temporal geometric accuracy is below the requirements. A map of regions with decreased multi-temporal geometric accuracy is presented in Figure 23.

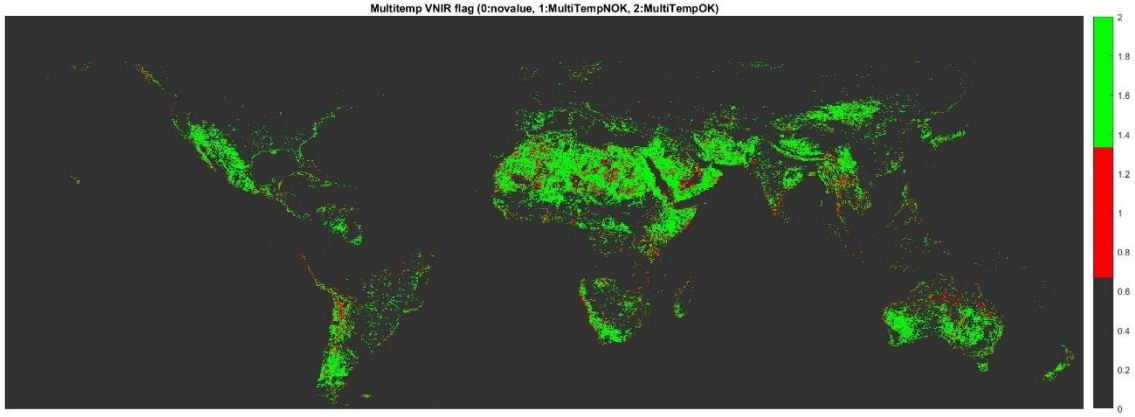

Figure 23: Multi-temporal geometric accuracy for the VNIR sensor for 16/12/2018 – 15/3/2019. Compliant areas are marked in green; areas with accuracy below 95% are marked in red. Grey areas represent no data.

For the combined VNIR/SWIR the multi-temporal geometric accuracy is compliant with the requirements. A map of regions with decreased multi-temporal geometric accuracy is presented in Figure 24.

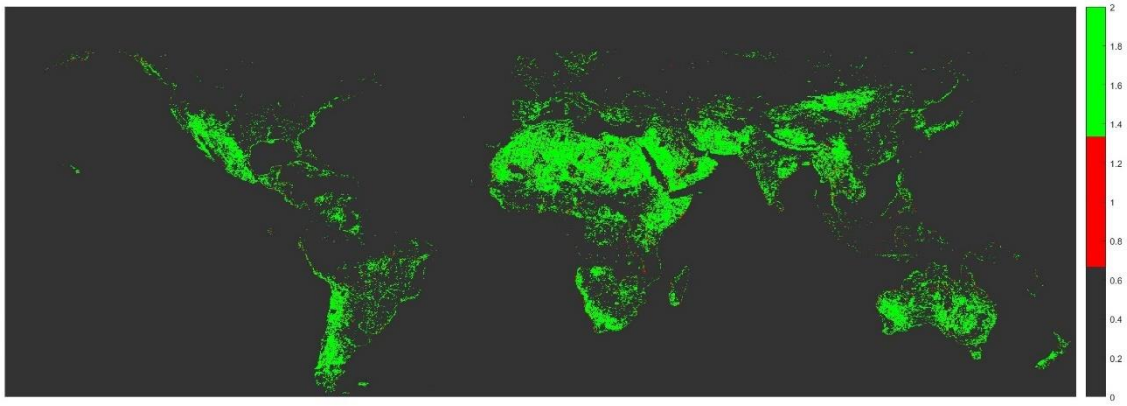

Figure 24: Multi-temporal geometric accuracy for the VNIR/SWIR combined for 16/12/2018 – 15/3/2019. Compliant areas are marked in green; areas with accuracy below 95% are marked in red. Grey areas represent no data.

Over the last full year, the multi-temporal accuracy for VNIR and VNIR/SWIR is 75.20% and 89.68%, respectively.

2.4. Geometric ICP file

On 08.09.2016 a new file with validity date set to 01.09.2016 was created.

ICP filename	Description
PROBAV_ICP_GEOMETRIC#LEFT_20160901_V01 PROBAV_ICP_GEOMETRIC#CENTER_20160901_V01 PROBAV_ICP_GEOMETRIC#RIGHT_20160901_V01	Correction for the gradual degradation observed in the last week of August and first week of September 2016.

3. Reference documents

RD-1	PROBA-V Commissioning Report Annex 1-Radiometric Calibration Results [N77D7-PV02-US-20-CRPT-Annex1-RadiometricCalibartion-v1_3]
RD-2	PROBA-V Commissioning Report Annex 2-Geometric Calibration Results [N77D7-PV02-US-20-CRPT-Annex2-GeometricCalibartion-v1_3]
LIT1	Govaerts Y., Sterckx S. and Adriaensen S. (2013) "Use of simulated reflectances over bright desert target as an absolute calibration reference" Remote Sensing Letters, Vol. 4, Iss. 6, 2013.
LIT2	S. Adriaensen, K. Barker, L. Bourg , M. Bouvet, B. Fougnie, Y. Govaerts, P. Henry, C. Kent, D. Smith, S. Sterckx. "CEOS IVOS Working Group 4: Intercomparison of vicarious calibration methodologies and radiometric comparison methodologies over pseudo-invariant calibration sites A Report to the CEOS/IVOS Working Group", 2012
LIT3	Sterckx S., Adriaensen S., Livens, L., "Rayleigh, Deep Convective Clouds and Cross Sensor Desert vicarious calibration validation for the PROBA-V mission." IEEE Transactions on Geoscience and Remote Sensing. Inter-Calibration of Satellite Instruments Special Issue. Vol.51:3, 1437 – 1452.

Table 18: Reference Documents